












The effect of the vertical gradients of photosynthetic parameters on the CO₂ assimilation and transpiration of a Panamanian tropical forest

Julien Lamour¹ , Kenneth J. Davidson^{1,2} , Kim S. Ely¹ , Gilles Le Moguédec³ , Jeremiah A. Anderson¹ , Qianyu Li¹ , Osvaldo Calderón⁴, Charles D. Koven⁵ , S. Joseph Wright⁴ , Anthony P. Walker⁶ , Shawn P. Serbin¹  and Alistair Rogers¹ 

¹Environmental & Climate Sciences Department, Brookhaven National Laboratory, Upton, NY 11973, USA; ²Department of Ecology and Evolution, Stony Brook University, Stony Brook, NY 11974, USA; ³AMAP, Université Montpellier, INRAE, Cirad CNRS, IRD, Montpellier 34000, France; ⁴Smithsonian Tropical Research Institute, Balboa 0843-03092, Republic of Panama; ⁵Climate and Ecosystem Sciences Division, Lawrence Berkeley National Laboratory, Berkeley, CA 94720, USA; ⁶Environmental Sciences Division and Climate Change Science Institute, Oak Ridge National Laboratory, Oak Ridge, TN 37831, USA

Summary

Author for correspondence:
Julien Lamour
Email: jlamour.sci@gmail.com

Received: 6 October 2022
Accepted: 14 March 2023

New Phytologist (2023) **238**: 2345–2362
doi: 10.1111/nph.18901

Key words: canopy height, climate change, leaf area index, leaf traits, photosynthesis, stomatal conductance, vertical gradients, water-use efficiency.

- Terrestrial biosphere models (TBMs) include the representation of vertical gradients in leaf traits associated with modeling photosynthesis, respiration, and stomatal conductance. However, model assumptions associated with these gradients have not been tested in complex tropical forest canopies.
- We compared TBM representation of the vertical gradients of key leaf traits with measurements made in a tropical forest in Panama and then quantified the impact of the observed gradients on simulated canopy-scale CO₂ and water fluxes.
- Comparison between observed and TBM trait gradients showed divergence that impacted canopy-scale simulations of water vapor and CO₂ exchange. Notably, the ratio between the dark respiration rate and the maximum carboxylation rate was lower near the ground than at the top-of-canopy, leaf-level water-use efficiency was markedly higher at the top-of-canopy, and the decrease in maximum carboxylation rate from the top-of-canopy to the ground was less than TBM assumptions.
- The representation of the gradients of leaf traits in TBMs is typically derived from measurements made within-individual plants, or, for some traits, assumed constant due to a lack of experimental data. Our work shows that these assumptions are not representative of the trait gradients observed in species-rich, complex tropical forests.

Introduction

Terrestrial biosphere models (TBMs) are our primary tool for modeling the exchanges of water vapor and carbon dioxide (CO₂), between the land surface and the atmosphere, and for projecting the responses of forests to climate change (Mitchard, 2018; Sullivan *et al.*, 2020; Gatti *et al.*, 2021). The rich diversity of plant species is necessarily simplified in TBMs, where plant diversity is collapsed into plant functional types (PFTs), usually *c.* 14 for the entire planet (Fisher *et al.*, 2015, 2018; Rogers *et al.*, 2017a; Franklin *et al.*, 2020). To enable PFTs to behave differently in TBMs, the processes which control CO₂ and water vapor exchange require PFT-specific parameterization. This is achieved by providing each PFT with a suite of top-of-canopy leaf traits.

The simulation of canopy-scale fluxes is derived from the simulation of mass and energy exchanges from leaves aggregated

across different canopy strata (Krinner *et al.*, 2005; Clark *et al.*, 2011; Rogers *et al.*, 2017a). Therefore, the upscaling from leaf to canopy requires a reliable description of how key leaf traits vary throughout the vertical profile of a canopy (Niinemets *et al.*, 2015).

Many studies have evaluated how carboxylation capacity normalized to 25°C ($V_{\text{cmax}25}$) and leaf nitrogen content expressed on a leaf area basis (N_a) vary within-individual plant canopy in concert with canopy gradients of irradiance (Field, 1983; Hirose & Werger, 1987; Chen *et al.*, 1993; Kull & Kruijt, 1999; Meir *et al.*, 2002; Lloyd *et al.*, 2010; Hikosaka, 2016). Results from this previous work – notably the optimal model of nutrient and photosynthetic traits distribution from Lloyd *et al.* (2010) – are used to scale $V_{\text{cmax}25}$ from the top of the forest canopy to the ground using an exponential decrease with either the leaf area index (LAI) or with the relative depth from the top-of-canopy (rd), that are both proxies for decreasing irradiance with canopy

depth (De Pury & Farquhar, 1997; Krinner *et al.*, 2005; Clark *et al.*, 2011; Oleson *et al.*, 2013; Rogers *et al.*, 2017a). Typically, the other photosynthetic parameters, maximum electron transport rate, triose phosphate utilization rate, and nonphotorespiratory respiration, all normalized to 25°C ($J_{\max 25}$, T_{p25} , $R_{\text{dark}25}$ respectively) are scaled proportionally with $V_{\text{cmax}25}$ using constant ratios (Krinner *et al.*, 2005; Clark *et al.*, 2011; Oleson *et al.*, 2013), implying that the vertical exponential decrease constant (k_n ; Lloyd *et al.*, 2010) is considered the same for all parameters.

In TBMs, the use of the equation presented by Lloyd *et al.* (2010), or obtained from other within-plant-models, to represent the photosynthetic gradients in forests implicitly assumes that within-plant gradients are the same as forest stand gradients. This assumption is not supported by Lloyd *et al.* (2010), who showed that the between-tree gradients of N_a were significantly different from the within-tree gradients. Therefore, using within-plant models to predict gradients in $V_{\text{cmax}25}$ in complex forests could cause bias due to the known stratification of different species along light gradients. Indeed, within-plant models cannot capture interspecific variation in functional traits. For example, the maximum and minimum leaf photosynthetic capacity and nutrient composition is species dependent (Reich *et al.*, 1995; Meir *et al.*, 2002; Osnas *et al.*, 2018) and could impact photosynthetic trait distribution.

So far, information on photosynthetic gradients in tropical forest canopies that include a mix of species is limited (Carswell *et al.*, 2000; Domingues *et al.*, 2005, 2014; Kumagai *et al.*, 2006; Cavaleri *et al.*, 2010; Kosugi *et al.*, 2012), and to our knowledge, the assumption that gradients of photosynthetic parameters in mixed species forest would follow the prediction of within-plant models has not been tested, potentially impacting predictions of carbon and water exchanges.

Another important component of modeling gas exchange is stomatal conductance (Ball *et al.*, 1987; Leuning, 1995; Medlyn *et al.*, 2011) and particularly the stomatal slope parameter, g_1 (Hetherington & Woodward, 2003; Franks *et al.*, 2018; Migliavacca *et al.*, 2021). The g_1 parameter represents the cost of CO₂ fixation in terms of water loss (Medlyn *et al.*, 2011) and has been shown to vary with species and growth environment (Hérault *et al.*, 2013; Lin *et al.*, 2015; Franks *et al.*, 2017; Wolz *et al.*, 2017; Wu *et al.*, 2020). Terrestrial biosphere models assume that g_1 is fixed throughout the vertical profile. This assumption has rarely been tested (Domingues *et al.*, 2014), and most studies seeking to understand variation in g_1 have focused on sunlit top-of-canopy leaves.

In this study, we evaluated the common TBM assumption that $V_{\text{cmax}25}$, $J_{\max 25}$, T_{p25} , and $R_{\text{dark}25}$ vary proportionally within the canopy that they scale proportionally with N_a , and follow an exponential decrease within the canopy. We also evaluated the assumption that g_1 is constant throughout the vertical profile. To evaluate these assumptions, we sampled leaves from all the species present at 10 heights in 10 vertical profiles within a Panamanian tropical forest. We supplemented traditional destructive chemical analyses and gas exchange measurements with spectroscopy, which enables rapid measurement of leaf traits, and an increased

data collection across multiple species (Serbin *et al.*, 2019; Burnett *et al.*, 2021; Lamour *et al.*, 2021d). Finally, to assess the impact of our observations on canopy-scale fluxes of CO₂ and water vapor, we compared fluxes modeled using our observed leaf trait gradients with fluxes modeled using the vertical gradients currently implemented for a broadleaf evergreen tropical (BET) forest PFT in the vegetation model 'Functionally Assembled Terrestrial Ecosystem Simulator' that is used in some TBMs (hereafter FATES; Fisher *et al.*, 2015; Koven *et al.*, 2020).

Materials and Methods

Study site and tree access

The study site was located in the San Lorenzo Forest in Colón Province, Panama (9.280°N, -79.975°W, 120 m above sea level), where the Smithsonian Tropical Research Institute operates a canopy access crane since 1997. The forest has escaped major anthropogenic disturbance for > 150 yr (Basset, 2003) and contains a large diversity of liana, epiphytes, and broadleaf evergreen trees reaching a maximum height of 40 m. The meteorological conditions on this site (Fig. 1a; Paton, 2022) are representative of humid tropical forests found in the Caribbean. Air temperature is stable throughout the year with an average of 25.5°C, and the rainfall totals > 3300 mm yr⁻¹. The data collection was performed during the dry season between January and April 2020.

Sampling design

Ten vertical profiles were identified within the 54 m radius of the crane boom. Candidate profiles needed to have access from the top-of-canopy to the ground and to be wide enough to fit the crane's 1.6 by 1.6 m gondola without damaging the surrounding branches. Each profile was divided into 10 height levels equidistant from the top-of-canopy to the ground. Level 1 corresponded to the top-of-canopy and level 10 a few meters above the ground (Fig. 2). At levels 1, 3, 5, 8, and 10, we cut one branch predawn and immediately put it into a bucket of water. Each branch was recut underwater and transferred to a shaded area. Both precautions were taken to avoid xylem cavitation and to protect shade-tolerant species from high irradiance in order to avoid impact on leaf gas exchanges (Santiago & Mulkey, 2003; Leakey *et al.*, 2006; Sperry, 2013; Verryckt *et al.*, 2020; Davidson *et al.*, 2022). Once on the ground, a mature leaf of each excised branch was used for direct measurement of the following leaf traits: $V_{\text{cmax}25}$, $J_{\max 25}$, $R_{\text{dark}25}$, T_{p25} , stomatal conductance to water vapor measured in dark-adapted leaves ($g_{\text{sw,dark}}$), the intercept parameter of stomatal models (g_0), g_1 , leaf mass per surface area (LMA), N_a , and leaf water content (LWC).

We made additional leaf reflectance measurements at all levels of the canopy (1–10; Fig. 2) between 08:00 and 17:00 h. At each level, we selected mature leaves from all the species that could be reached from the gondola. In total, 57 species were measured (Supporting Information Table S1). The reflectance spectra measured on those leaves allowed us to predict photosynthetic and structural traits ($V_{\text{cmax}25}$, $J_{\max 25}$, $R_{\text{dark}25}$, T_{p25} , LMA, N_a , and

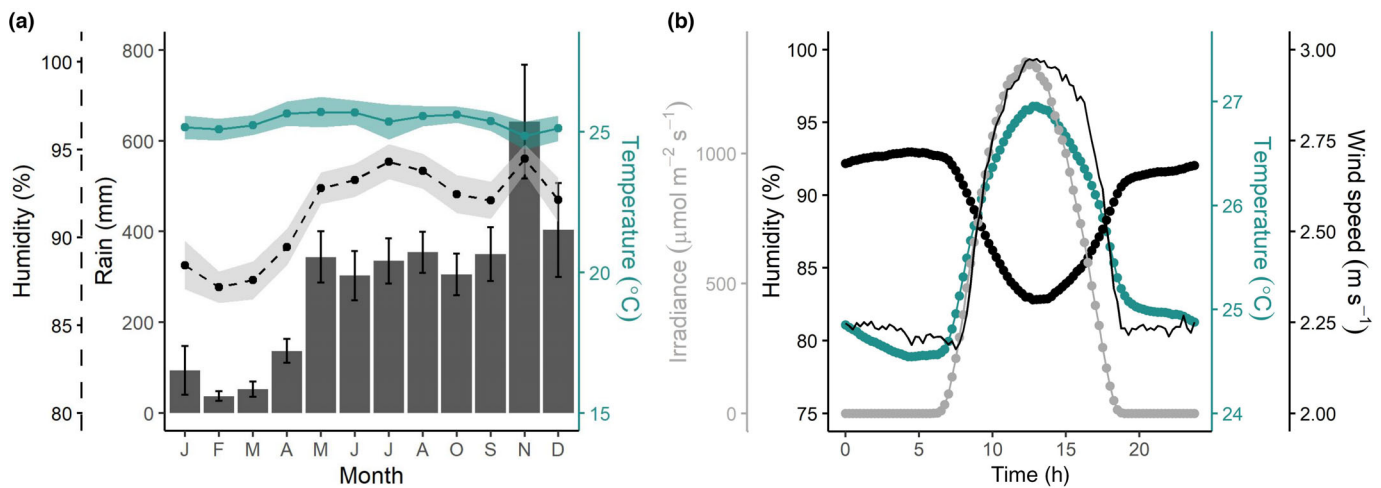


Fig. 1 Meteorological conditions at San Lorenzo Forest during the 2010–2020 period. (a) Monthly average of relative humidity (dark circles), air temperature (green circles), and precipitation (bars). (b) Average variation in meteorological conditions over a 24 h period during the dry season (January–April) with the photosynthetically active irradiance (gray), relative humidity (black), temperature (green), and wind speed (black line). The envelopes and the error bars in panel (a) represent the confidence interval of the mean. The data collection was performed from January to April 2020.

LWC). The traits measured using traditional approaches (e.g. gas exchange and leaf chemical analysis) were used to evaluate the performance of the spectra–trait models on independent observations (Fig. 3) and, where necessary, to improve spectra–trait models (Lamour *et al.*, 2021d). Analysis of trait gradients is based upon the high-resolution, species-rich, spectra-derived datasets with the exception of the gradients of stomatal conductance parameters, g_0 , $g_{sw, dark}$, and g_1 , that could not be estimated from reflectance data because we do not have spectra–trait models for these fluxes and traits.

Vegetation structure and indices of vertical position

The vertical position (z) inside the canopy was described by the height above ground (h , in meters) and by the relative depth from the top canopy, rd (Eqn 1, $rd = 0$ at the top-of-canopy and $rd = 1$ on the ground; Fig. 2):

$$rd = \frac{H-h}{H} \quad \text{Eqn 1}$$

where H (in meters) corresponds to the height at the top-of-canopy for each vertical profile.

We also measured the cumulative LAI at the 10 levels of seven of the 10 vertical profiles (campaign cut short due to COVID-19) using two paired LAI-2200C plant canopy analyzers (Li-Cor Biosciences, Lincoln, NE, USA), one above the canopy with an unobstructed view of the sky, and one within the canopy (Serbin *et al.*, 2009; Parker, 2020). Both sensors used a view restrictor cap of 90°.

Gas exchange measurements

Three types of gas exchange measurements were made using five LI-6400XT Portable Photosynthesis Systems and one LI-6800 Portable Photosynthesis System (Li-Cor Biosciences). First, a

photosynthetic light response ($A-Q$) curve was measured to identify the saturating irradiance of each leaf. Second, we performed a photosynthetic CO_2 response ($A-C_i$) curve where the CO_2 at the leaf surface was varied to modulate the intercellular CO_2 concentration (C_i), at saturating irradiance. Finally, the leaf dark respiration rate (R_{dark}) was measured after 45 min of acclimation in the dark. The gas exchange measurements were made between 06:00 and 18:00 h the same day we cut the branches. The approach used for these three measurements followed established methods (Long & Bernacchi, 2003; Rogers *et al.*, 2017b) with full details to be found in Lamour *et al.* (2021d).

Estimation of photosynthetic traits From each $A-C_i$ curve, the parameters V_{cmax} , J_{max} , and T_p were estimated based on the equations of the FvCB model (Farquhar *et al.*, 1980). The resulting parameters were then scaled to a common reference temperature of 25°C using the temperature dependences used in FATES (Leuning, 2002; Bernacchi *et al.*, 2003) as summarized by Bonan *et al.* (2011, table B3) and described in detail previously (Lamour *et al.*, 2021d).

Estimation of conductance traits The first point of the $A-Q$ and $A-C_i$ curves corresponded to a stable measurement of A and g_{sw} achieved after a minimum of 20 min of acclimation to the conditions inside the gas exchange instruments (Rogers *et al.*, 2017b; Lamour *et al.*, 2021d), and notably to the leaf to air water vapor pressure deficit (VPD_{leaf} , 1.3 ± 0.20 SD, kPa) and the CO_2 concentration at the leaf surface (CO_{2s} , 398 ± 2 SD, ppm). We used those points to estimate the conductance parameters of the USO model (Medlyn *et al.*, 2011; Eqn 2):

$$g_{sw} = g_0 + 1.6 \left(1 + \frac{g_1}{\sqrt{VPD_{leaf}}} \right) \frac{A}{CO_{2s}} \quad \text{Eqn 2}$$

where g_0 is the intercept of the model for $A=0$, and g_1 is the slope of the model.

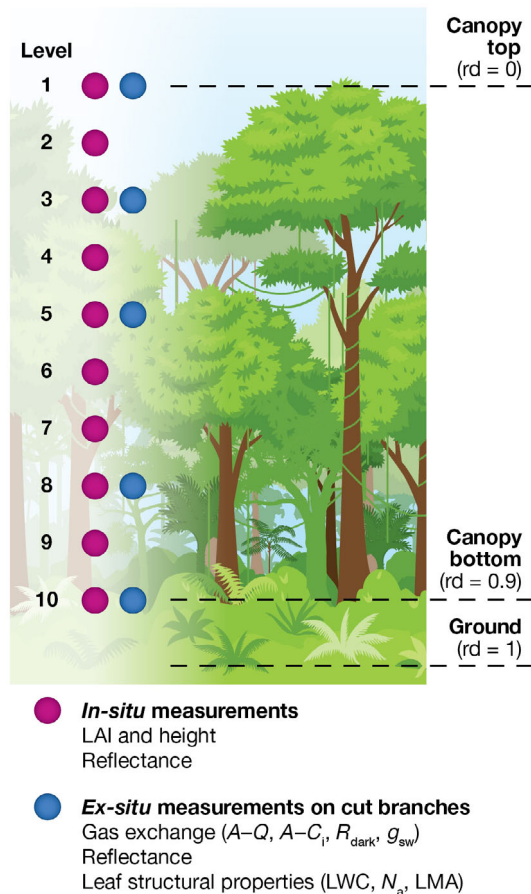


Fig. 2 Description of the measurements made on the vertical profiles. Level 1 corresponds to the top of the canopy for a given vertical profile. Level 10 corresponds to the lowest canopy level set at 1/10 of the total vertical profile height. rd represents the relative depth from top-of-canopy. At each magenta point, mature leaves from all the species that could be reached from the crane gondola were measured for reflectance. The reflectance spectra were subsequently used to predict key leaf traits using spectroscopy models. The vertical variation of these traits is analyzed in this study. At each blue point, one branch was cut predawn and immediately immersed and recut in water to avoid embolism. One mature leaf was then measured on the ground using traditional approaches (e.g. gas exchange). Those values were used to validate and build the spectroscopy models.

Eqn 2 was rearranged into a linear form (Eqn 3) where X is the USO regressor and Y is the response variable. This rearrangement of the equation allowed us to use linear regressions to estimate g_0 and g_1 (Lamour *et al.*, 2022):

$$Y = g_0 + g_1 X \quad \text{Eqn 3}$$

$$X = \frac{1.6A}{\sqrt{\text{VPD}_{\text{leaf}} \text{CO}_{2s}}} \quad \text{Eqn 4}$$

$$Y = g_{\text{sw}} - \frac{1.6A}{\text{CO}_{2s}} \quad \text{Eqn 5}$$

The dark-adapted measurement of R_{dark} also provided a measurement of g_{sw} in a dark-adapted leaf ($g_{\text{sw,dark}}$).

Leaf structural measurements

LMA, LWC, and N_a were measured after the completion of the gas exchange measurements. Disks of known area were sampled from the leaves and weighed before being oven-dried at 70°C to a constant mass. The fresh and dry weights were used to calculate LMA and LWC. Dried leaves were subsequently ground, and elemental nitrogen was quantified using a 2400 Series II CHN analyzer following the manufacturer's instructions (PerkinElmer, Waltham, MA, USA).

Estimating physiological traits with spectroscopy

The reflectance of leaves on excised branches was measured using a Spectral Evolution PSR+ 3500 (spectral range: 350–2500 nm; Spectral Evolution, Haverhill, MA, USA) spectroradiometer together with an external light source mounted in a leaf clip with a black background (SVC LC-RP-Pro foreoptic; Spectra Vista Corp., Poughkeepsie, NY, USA). The leaf reflectance of attached leaves within the vertical profiles (Fig. 2) was measured using the SVC HR-1024i with an attached LC-RP-Pro leaf clip. Three to four reflectance measurements were made on different sections of the leaf. They were then averaged account for within-leaf heterogeneity. All subsequent analyses were based on this average reflectance.

To predict the LMA, we used the partial least squares regression (PLSR) model from Serbin *et al.* (2019), which was trained using observations from multiple biomes, including measurements made at the San Lorenzo study site. The model had shown a good accuracy ($R^2 = 0.89$, RMSE = 15.45 g m⁻²), which was comparable when applied to the reference data acquired for this study ($R^2 = 0.89$, RMSE = 17.8 g m⁻²; Fig. 3a). However, a bias was found between the predicted and the observed LMA and was corrected for this study using a linear regression (Fig. 3a).

N_a prediction was done by building a new PLSR model trained using data from various datasets (Table S2). This model had a low RMSE of 0.31 g m⁻² and R^2 of 0.85 when validated against the independent observations taken in this study (Fig. 3b). LWC was also predicted using a new PLSR model trained using diverse datasets (Table S2) and had a R^2 and RMSE of 0.84 and 2.88%, respectively, on the independent data from this study (Fig. 3c).

The traits $V_{\text{cmax}25}$, $J_{\text{max}25}$, $R_{\text{dark}25}$, and $T_{\text{p}25}$ were predicted using the PLSR models published by Lamour *et al.* (2021d). The models were trained using data from several years and multiple sites and included the data obtained for this study. They showed good predictive performance for $V_{\text{cmax}25}$, $J_{\text{max}25}$, $T_{\text{p}25}$, and $R_{\text{dark}25}$ on independent observations (RMSE of 13.4, 19.9, 1.5, and 0.3 μmol m⁻² s⁻¹, and R^2 of 0.74, 0.73, 0.64, and 0.58, respectively; Lamour *et al.*, 2021d).

Importantly, the error associated with trait predictions using spectra was not related to vertical position (no trend or heteroscedasticity), so it was possible to use such models to study the vertical gradients.

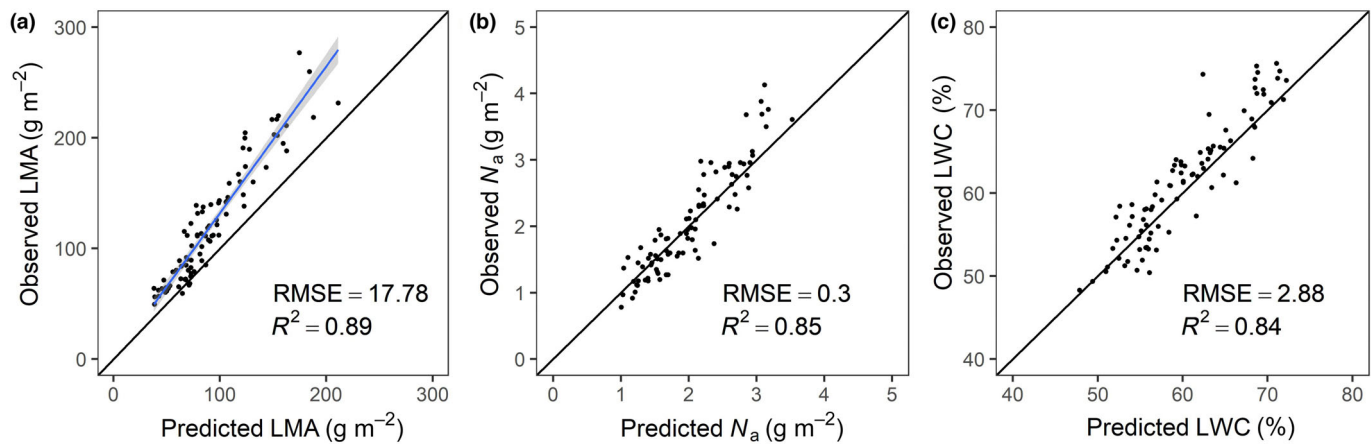


Fig. 3 Observed vs predicted values obtained using spectra–trait partial least squares regression (PLSR) models tested against the independent observations from this study. The PLSR model for leaf mass per surface area (LMA) prediction was from Serbin *et al.* (2019) (a) and showed a bias (blue line), which was corrected for the prediction in the rest of the study. The nitrogen content per surface area (N_a) and the leaf water content (LWC) prediction were made using PLSR models built using observations from several datasets (Supporting Information Table S2) (b, c). The black line corresponds to the 1 : 1 line.

Statistical analysis

We used mixed models with the vertical profile (v) as random factor to describe the parameter (P) variation within the vertical profiles. We used linear (Eqn 6), quadratic (Eqn 7), and exponential models (Eqn 8) associated with the variation in z . The linear equation is the simplest model of vertical variability, the quadratic equation allows the representation of more complex vertical variation and finally, the exponential model is the model commonly used in TBMs to represent the variation in LMA, N_a , $V_{\text{cmax}25}$, $J_{\text{max}25}$, and $R_{\text{dark}25}$.

To study the fixed structure of the models and compare them, we analyzed the residuals as well as their Akaike information criterion (AIC; Akaike, 1974). Statistical analysis were performed in R (R Core Team, 2020). The models were fit using the maximum likelihood method, which is suitable for comparing fixed structures of mixed models, using the package NLME and the associated textbook (Pinheiro & Bates, 2000):

$$P_{v,i} = a + \alpha_v + (b + \beta_v)z_{v,i} + \epsilon_{v,i} \quad \text{Eqn 6}$$

$$P_{v,i} = a + \alpha_v + (b + \beta_v)z_{v,i} + cz_{v,i}^2 + \epsilon_{v,i} \quad \text{Eqn 7}$$

$$P_{v,i} = (a + \alpha_v)e^{-(b+\beta_v)z_{v,i}} + \epsilon_{v,i} \quad \text{Eqn 8}$$

where i is the i^{th} measurement made on vertical profile v , a is the intercept of the models, α_v is the random effect of v on a , $\alpha_v \sim N(0, \sigma_a^2)$, b is the fixed effect of z , β_v is the random effect of v on b , $\beta_v \sim N(0, \sigma_\beta^2)$, c is the fixed effect associated with the quadratic term z^2 and $\epsilon_{v,i}$ is the residual, $\epsilon_{v,i} \sim N(0, \sigma^2)$. Note that the b parameter of the exponential model (Eqn 8) is also referred to as k_n .

We tested which of the three vertical indices (rd, LAI, and h) best predicted P by comparing the AIC of the models and limited this analysis to the seven vertical profiles that were measured for LAI.

We checked whether the ratio between $J_{\text{max}25}$, T_{p25} , $R_{\text{dark}25}$, and $V_{\text{cmax}25}$ was constant inside the canopy using Eqns 6, 7 where P corresponded to the ratio. We used the same approach to test whether the ratio between $V_{\text{cmax}25}$, $J_{\text{max}25}$, T_{p25} , $R_{\text{dark}25}$, and N_a was constant vertically.

We investigated whether the conductance parameters g_0 and g_1 of the USO conductance model were constant vertically using Eqn 9 where the random effect of the leaf sample (s) is applied to account for the fact that multiple measurements were taken on the same leaves (first point from the $A-C_i$ and $A-Q$ curves). For simplicity, we did not include a random vertical profile effect as the vertical profile variation on both g_0 and g_1 was low compared with the sample-to-sample variation and because the number of leaf measurements was relatively low (77 leaves):

$$Y_{s,i} = g_0 + az_s + \alpha_s + (g_1 + bz_s + \beta_s)X_{s,i} + \epsilon_{s,i} \quad \text{Eqn 9}$$

where i is the i^{th} measurement made on s , a is the fixed effect of z on g_0 , α_s is the random effect associated with s on g_0 , $\alpha_s \sim N(0, \sigma_a^2)$, b is the fixed effect of z_s on g_1 , β_s is the random slope effect factor associated with s , $\beta_s \sim N(0, \sigma_\beta^2)$, and $\epsilon_{s,i}$ is the residual of the model, $\epsilon_{s,i} \sim N(0, \sigma^2)$.

Assessment of the effect of vertical gradients in gas exchange parameters on model predictions of canopy-scale H_2O and CO_2 fluxes

We used a canopy-scale gas exchange model which mimics the FATES core features, including photosynthesis, respiration, stomatal conductance, energy balance, and canopy scaling. For this, we used the R package LEAFGASEXCHANGE (Lamour & Serbin, 2021), which allows gas exchanges to be simulated at the leaf level and to be scaled to the canopy level using a description of the canopy structure and a light radiation-interception model (Bonan, 2019). Leaf scale photosynthesis follows the

FvCB model of photosynthesis which is coupled with the USO conductance model (Eqn 2). A minimum threshold, g_{sw} is equal to $g_{sw, dark}$, is used to avoid negative g_{sw} when $A < 0$ (Eqn 2). In addition, the leaf energy balance, necessary to calculate the leaf temperature, is simulated using the package TEALEAVES (Muir, 2019). We used the Norman (1979) radiation model implemented by Bonan (2019) to calculate the irradiance inside the canopy. This approach allowed us to simulate the irradiance at 20 heights inside the canopy for sunlit leaves which receive direct and diffuse irradiance, and for shaded leaves that only receive a diffuse source of irradiance. For this study, we used the average LAI of 6.2 measured at the site. We assumed that the wind speed followed an exponential decrease with LAI within the canopy (Buckley *et al.*, 2014).

We used the weather data from the on-site meteorological station to calculate the average hourly weather data for the dry season by averaging the first 4 months of the 10 previous years (Fig. 1b). The hourly humidity, radiation, temperature, and wind speed were used to drive the gas exchange predictions. We used dry season weather conditions as input of the simulations to be consistent with our measurements of leaf trait gradients that were made during the dry season and that may differ in the wet season. Subsequently, we estimated leaf gas exchange at all heights in the canopy for sunlit and shaded leaves and integrated the values over the entire canopy to estimate canopy-scale carbon assimilation (A) and transpiration (T).

Eight different scenarios of vertical gradient parametrization were investigated to test their impact on the canopy-scale fluxes. The first scenario corresponded to current default FATES parametrization for a BET forest. The subsequent scenarios corresponded to the progressive update of the parametrization to correspond more closely to our observations, with the last being the most complex with the greatest similarity to the gradients measured in the forest. (1) FATES default parametrization for a BET; (2) FATES parametrization adapted to the site, that is, top-of-canopy photosynthesis traits V_{cmax25} , J_{max25} , and R_{dark25} were set to the measured values. k_n was derived following Lloyd *et al.* (2010) as in FATES:

$$\log(k_n) = 0.00963 V_{cmax25} - 2.43 \quad \text{Eqn 10}$$

(3) k_n was replaced by the measured value for V_{cmax25} and used for the three parameters V_{cmax25} , J_{max25} , and R_{dark25} . (4) k_n was adapted to its measured values for R_{dark25} . (5) The observed photosynthetic gradients were used (contrary to scenario 4, we used the equation with the lowest AIC among Eqns 6, 7, or 8 to describe V_{cmax25} , J_{max25} , and R_{dark25} variation). (6) Conductance traits were set to their values measured on this site (g_0 , g_1 , and $g_{sw, dark}$) in place of FATES default parametrization. (7) Measured vertical gradients of g_1 were used. (8) In all the previous scenarios, we considered that the triose phosphate utilization (TPU) was never limiting photosynthesis in the FvCB model (McClain & Sharkey, 2019; Gregory *et al.*, 2021; Rogers *et al.*, 2021). We checked this assumption by adding a TPU limitation using estimated gradients of T_{p25} obtained on this site and comparing this scenario with the previous one.

Results

Vertical gradients of leaf traits

Canopy height (H) varied between 18.2 and 33.6 m with a mean of 25.8 ± 1.2 m (Fig. 4; mean \pm SE). Leaf area index at the top-of-canopy for each vertical profile was close to zero (0.4 ± 0.1) but could have higher values if taller neighbor trees were in view of the sensor. Total canopy LAI measured near the ground ($rd = 0.9$) ranged between 4.70 and 8.64 with a mean of 6.2 ± 0.5 . Interestingly, the tallest vertical profile also had the lowest total canopy LAI (Fig. 4b) and the total LAI was negatively correlated with the height of the vertical profile. In general, LAI increased linearly along the vertical profile from the top-of-canopy to the ground.

Leaf composition and photosynthetic traits were variable vertically (Figs 5, 6; Table 1). rd best explained the vertical variation of the photosynthetic parameters and N_a (lowest AIC for each trait; Tables S3, S4). For LMA and LWC, h was a better descriptor (Table S3), but using rd or h led to the same formulation to

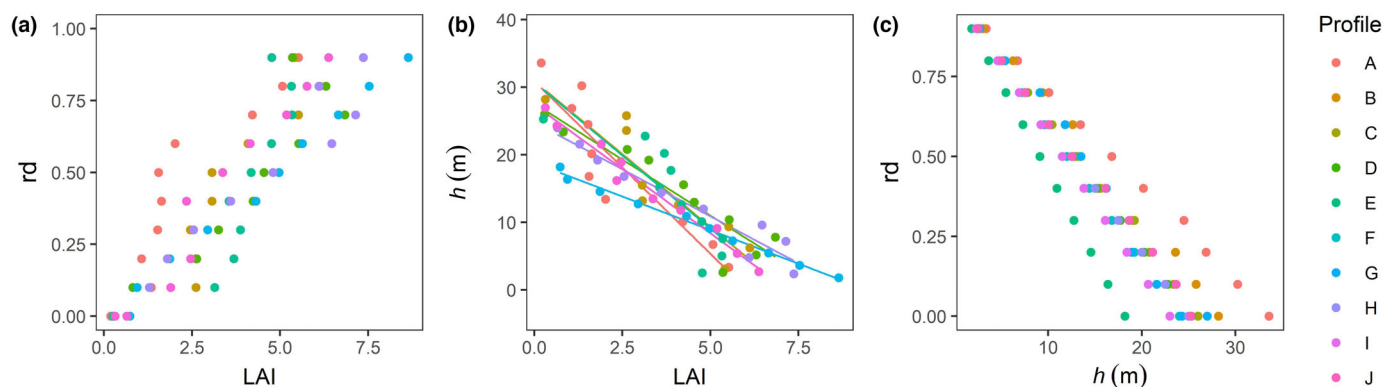


Fig. 4 Relationship between the different indices of verticality, (a) LAI (leaf area index) and rd (relative depth from the top of the canopy), (b) LAI and h (height), (c) rd and h . Each vertical profile (A–J) is represented by a different color. LAI was measured in only seven profiles (A–G). In panel (b), the lines represent the linear regression between LAI and h . The slope of the regression was negatively correlated with the height at the top of the canopy of the vertical profiles (P -value < 0.01).

describe their vertical gradient (exponential variation for LMA Eqn 8, quadratic equation for LWC Eqn 7; Table S3). We therefore describe the variation of P with rd hereafter. Note that among the z indices, LAI was consistently the worst metric at describing the vertical variation (Table S3). At our site and as expected, rd and LAI were highly correlated ($r=0.89$) but the LAI measured near the ground ($rd=0.9$) varied markedly between vertical profiles with values ranging from 4.70 to 8.64. Leaf area index did not explain the variation of the photosynthetic traits measured at this level ($P>0.05$, not shown).

Leaf mass per surface decreased exponentially with values approximately twice as high at the top-of-canopy as near the ground (189 ± 14 vs 89 ± 4 g m^{-2} ; Fig. 5a,b; Table 1). N_a was also higher at the top-of-canopy (3.09 ± 0.15 vs 1.88 ± 0.08 ; Fig. 5c,d; Table 1), and its decrease with rd was best represented by a quadratic model (Eqn 7) with a concave shape. LWC had

lower values at the top-of-canopy and increased with rd (55.9 ± 1.4 vs 66.74 ± 1.0 ; Fig. 5e,f; Table 1).

The photosynthetic parameters $V_{\text{cmax}25}$, $J_{\text{max}25}$, $R_{\text{dark}25}$, and $T_{\text{p}25}$ decreased from the top-of-canopy to the ground (Fig. 6; Table 1). $V_{\text{cmax}25}$ and $J_{\text{max}25}$ varied in a similar way to N_a with a slope of decrease which was zero at the top-of-canopy ($b=0$; Table 1) and higher near the ground ($c<0$; Table 1). $R_{\text{dark}25}$ variation was best described by a linear model, and $T_{\text{p}25}$ with a quadratic model with a convex shape (Table 1).

All the traits showed strong horizontal variability, that is, a strong variation for a given rd position (Figs 5, 6). This was due to both variation within a given profile (Figs 7, S1–S6) and variation among profiles as shown by the relatively high standard deviation of the random effects (σ , σ_α , and σ_β ; Table 1) compared with the values of the fixed effect (a , b , and c ; Table 1). In addition, for most traits, the rate of change

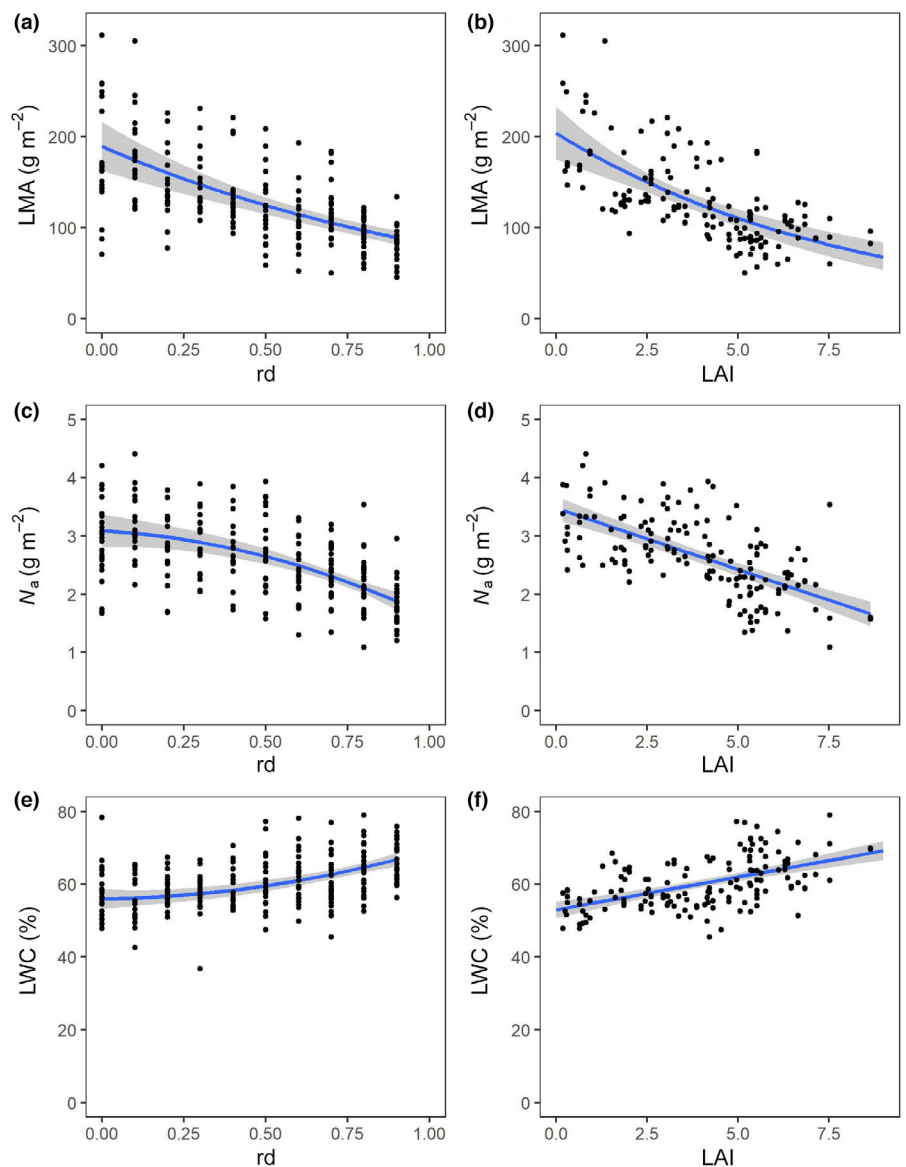


Fig. 5 Vertical gradients of leaf traits; leaf mass area (LMA) (a, b), leaf nitrogen content expressed per unit leaf area (N_a) (c, d), and leaf water content (LWC) (e, f). Left-hand panels (a, c, e) show leaf traits plotted against relative depth from top of the canopy (rd) and right-hand panels (b, d, f) show the data plotted against leaf area index (LAI). Each black point represents an estimation of a leaf trait (LMA, N_a , and LWC) by the spectroscopic models presented in Fig. 3. The blue lines and gray shaded area represent the mean value and its confidence interval estimated by the model with the lowest Akaike information criterion for each variable in Table 1.

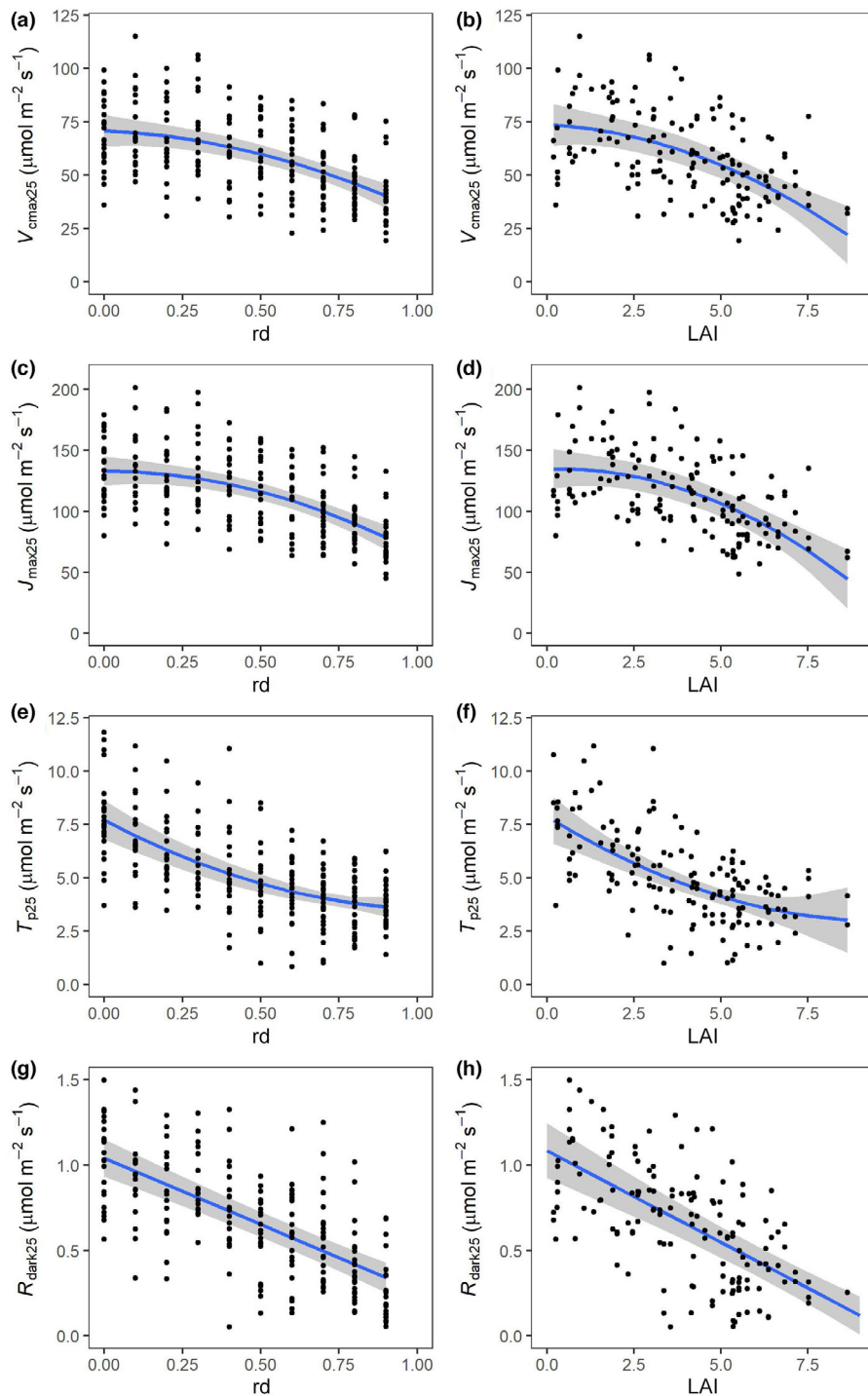


Fig. 6 Vertical gradients of photosynthetic parameters normalized to 25°C, the maximum carboxylation capacity ($V_{\text{cmax}25}$) (a, b), maximum electron transport rate ($J_{\text{max}25}$) (c, d), triose phosphate utilization rate ($T_{\text{p}25}$) (e, f), and the nonphotorespiratory respiration rate ($R_{\text{dark}25}$) (g, h). Left-hand panels (a, c, e, g) show leaf traits plotted against relative depth from top of the canopy (rd) and right-hand panels (b, d, f, h) show the data plotted against leaf area index (LAI). Each black point represents an estimation of a photosynthetic trait by the spectroscopic models presented by Lamour *et al.* (2021d). The blue lines and gray shaded area represent the mean value and its confidence interval estimated by the model with the lowest Akaike information criterion for each variable in Table 1.

in values from the top to the bottom of the canopy varied considerably among profiles (Fig. 7), but typically converged on a consistent value near the ground (Fig. 7; $V_{\text{cmax}25} = 39.5 \pm 2.6 \mu\text{mol m}^{-2} \text{s}^{-1}$). This was also the case for the other photosynthetic parameters and for LMA and N_a (Figs S1–S5). As a result, we tended to observe that each trait showed a consistent threshold in their values that was similar across all profiles, and this occurred at the highest relative canopy depths (rd = 0.9).

We evaluated whether the ratios between $J_{\text{max}25}$, $T_{\text{p}25}$, $R_{\text{dark}25}$, and $V_{\text{cmax}25}$ were influenced by the position within the canopy (Table 2; Fig. S7). The ratio $J_{\text{max}25} : V_{\text{cmax}25}$ was constant with canopy position at 1.96 ± 0.02 . However, the ratio between $R_{\text{dark}25}$ or $T_{\text{p}25}$ and $V_{\text{cmax}25}$ changed vertically. At the top-of-canopy, $R_{\text{dark}25} : V_{\text{cmax}25}$ was of 0.015 ± 0.001 (Table 2) and declined linearly to approximately half near the ground (0.008 ± 0.001 for rd = 0.9; Table 2). For $T_{\text{p}25} : V_{\text{cmax}25}$, the vertical structure was best described by a quadratic model that predicted the

Table 1 Vertical variation in leaf traits (*P*).

<i>P</i>	Eqn	<i>a</i>	σ_a	<i>b</i>	σ_b	<i>c</i>	σ	AIC
LMA	6	182.9*** ± 11.5	33.7	-112.4*** ± 15.2	42.0	-	31.1	2290
	7	185.9*** ± 12.1	33.9	-134.7*** ± 30.2	42.4	24.5 ^{ns} ± 28.6	31.0	2291
	8	189.3*** ± 13.7	40.8	-0.84*** ± 0.10	0.26	-	30.5	2285
<i>N_a</i>	6	3.23*** ± 0.14	0.39	-1.35*** ± 0.19	0.48	-	0.50	364
	7	3.09*** ± 0.15	0.37	-0.31 ^{ns} ± 0.45	0.47	-1.14* ± 0.45	0.49	360
	8	3.25*** ± 0.16	0.44	-0.49*** ± 0.07	0.18	-	0.50	367
LWC	6	54.5*** ± 1.3	3.0	12.2*** ± 1.7	3.0	-	6.2	1530
	7	55.9*** ± 1.4	2.9	1.4 ^{ns} ± 5.4	2.8	11.8* ± 5.7	6.2	1528
	8	54.5*** ± 1.2	2.9	0.21*** ± 0.03	0.05	-	6.2	1530
<i>V_{cmax25}</i>	6	74.6*** ± 3.5	9.3	-34.2*** ± 5.1	11.9	-	14.7	1939
	7	70.9*** ± 3.8	9.1	-6.7 ^{ns} ± 13.2	12.1	-30.3* ± 13.4	14.5	1936
	8	74.9*** ± 3.7	9.6	-0.54*** ± 0.08	0.19	-	14.8	1943
<i>J_{max25}</i>	6	141.2*** ± 5.7	15.1	-61.1*** ± 8.8	21.7	-	23.2	2155
	7	133.0*** ± 6.1	14.8	0.2 ^{ns} ± 21.0	22.1	-67.6** ± 21.1	22.7	2147
	8	141.7*** ± 5.9	15.3	-0.51*** ± 0.07	0.18	-	23.5	2160
<i>T_{p25}</i>	6	7.28*** ± 0.45	1.28	-4.48*** ± 0.59	1.51	-	1.50	878
	7	7.72*** ± 0.47	1.25	-7.76*** ± 1.37	1.48	3.60** ± 1.36	1.48	873
	8	7.53*** ± 0.46	1.26	-0.86*** ± 0.08	0.14	-	1.50	874
<i>R_{dark25}</i>	6	1.04*** ± 0.06	0.15	-0.78*** ± 0.07	0.17	-	0.21	-15.36
	7	1.01*** ± 0.06	0.16	-0.54** ± 0.20	0.19	-0.27 ^{ns} ± 0.20	0.21	-15.08
	8	1.07*** ± 0.06	0.15	-1.08*** ± 0.11	0.24	-	0.22	-8.48

a represents the intercept of the model, that is, *P* at the top of the canopy. σ_a is the SD associated with the random vertical profile effect (*v*) on *a*. *b* is the coefficient associated with the relative depth from the top-of-canopy (*rd*) and σ_b is the SD of the random effect of *v* on *b*. *c* represents the coefficient associated with *rd*² and σ is the SD of the residual. The values after the sign ± represent the SE of the estimation. *, *P* < 0.05; **, *P* < 0.01; ***, *P* < 0.001; AIC, Akaike information criterion; ns, not significant.

highest value at the top-of-canopy (0.115 ± 0.01; Table 2) and the lowest value in the mid-canopy (0.09 ± 0.005 for *rd* = 0.5).

Similarly, we evaluated whether the ratio between the photosynthetic parameters *V_{cmax25}*, *J_{max25}*, *R_{dark25}*, and *T_{p25}* and *N_a* was variable within the canopy (Table 2; Fig. S8). The ratio was constant for *V_{cmax25}* and *J_{max25}* and varied vertically for *R_{dark25}* and *T_{p25}*. The leaves of the lower part of the canopy had a ratio between *R_{dark25}* and *N_a* two times lower than sunlit leaves (0.36 ± 0.02 μmol g⁻¹ s⁻¹ for *rd* = 0 vs 0.18 ± 0.02 μmol g⁻¹ s⁻¹ for *rd* = 0.9).

Vertical patterns in measured leaf conductance traits were also analyzed. Conductance measured after a period of dark acclimation (*g_{sw,dark}*) was constant vertically (0.013 ± 0.002 mol m⁻² s⁻¹). *g₀* was not significantly different from zero and was not impacted by *z* (Table 3). Stomatal slope (*g₁*) displayed vertical structuring, with higher values near the ground than at the top-of-canopy (*b* = 1.13 ± 0.5; Table 3; Fig. S9). The variable *b* best explained variation in *g_{sw}* (lowest AIC; Table 3).

Impact of the gas exchange parameter vertical gradients on canopy-scale CO₂ assimilation and transpiration simulations

We provide an example of diurnal canopy gas exchange simulations in Fig. 8 corresponding to scenario 7 (Table 4) that considered the empirical gradients of photosynthetic and conductance traits observed in this forest. Maximum *A* and *g_{sw}* were simulated between 09:00 and 10:00 h at the top-of-canopy when the irradiance and humidity were high and the leaf temperature moderate.

As expected, simulated *A* and *g_{sw}* were also highly variable vertically (Fig. 8) and the top three layers of the canopy, that represented 15% of the total number of layers, were responsible for 47% and 36% of the total CO₂ assimilated and water transpired by the leaves summed over the whole canopy over 24 h.

Canopy-scale CO₂ assimilation (*A*) and transpiration (*T*) fluxes are presented in Table 4 for each scenario of vertical gradients. The values of the different scenarios (Table 4; Fig. S10) can be used to estimate the effect of the different simplifying assumptions that are usually made in TBMs. Using the site top-of-canopy values for *V_{cmax25}*, *J_{max25}*, and *R_{dark25}* as well as *k_n* (Eqn 10) was critical and increased *A* by 17% (scenario 2 vs scenario 1). Adapting *k_n* so it corresponded to the values measured for *V_{cmax25}* had a low overall impact on *A* and changed it by 3% (scenario 3 vs scenario 2). However, when the site *k_n* was used for *R_{dark25}*, *A* increased by 13% (scenario 4 vs scenario 3) as a result of lower *R_{dark}* in the understory (Fig. S10). Using the best model fit to represent the gradients in *V_{cmax25}*, *J_{max25}*, and *R_{dark25}* only marginally impacted *A* compared with using an exponential decrease with a *k_n* adapted to the site (scenario 5 vs scenario 4). Overall, considering the default photosynthesis parametrization for the site (scenario 2) compared with the measured gradients (scenario 5) changed *A* by 12%.

Using the measured *g₁* in place of the default *g₁* had a limited effect on *A* (-6%) but markedly impacted *T* (-22%, scenario 6 vs scenario 5; Table 4). The addition of *g₁* variation with *rd* (Table 4) increased *T* by 21% as a result of increasing *g_{sw}* inside the canopy (scenario 7 vs scenario 6; Table 4). The effect on *A* was however limited (+4%).

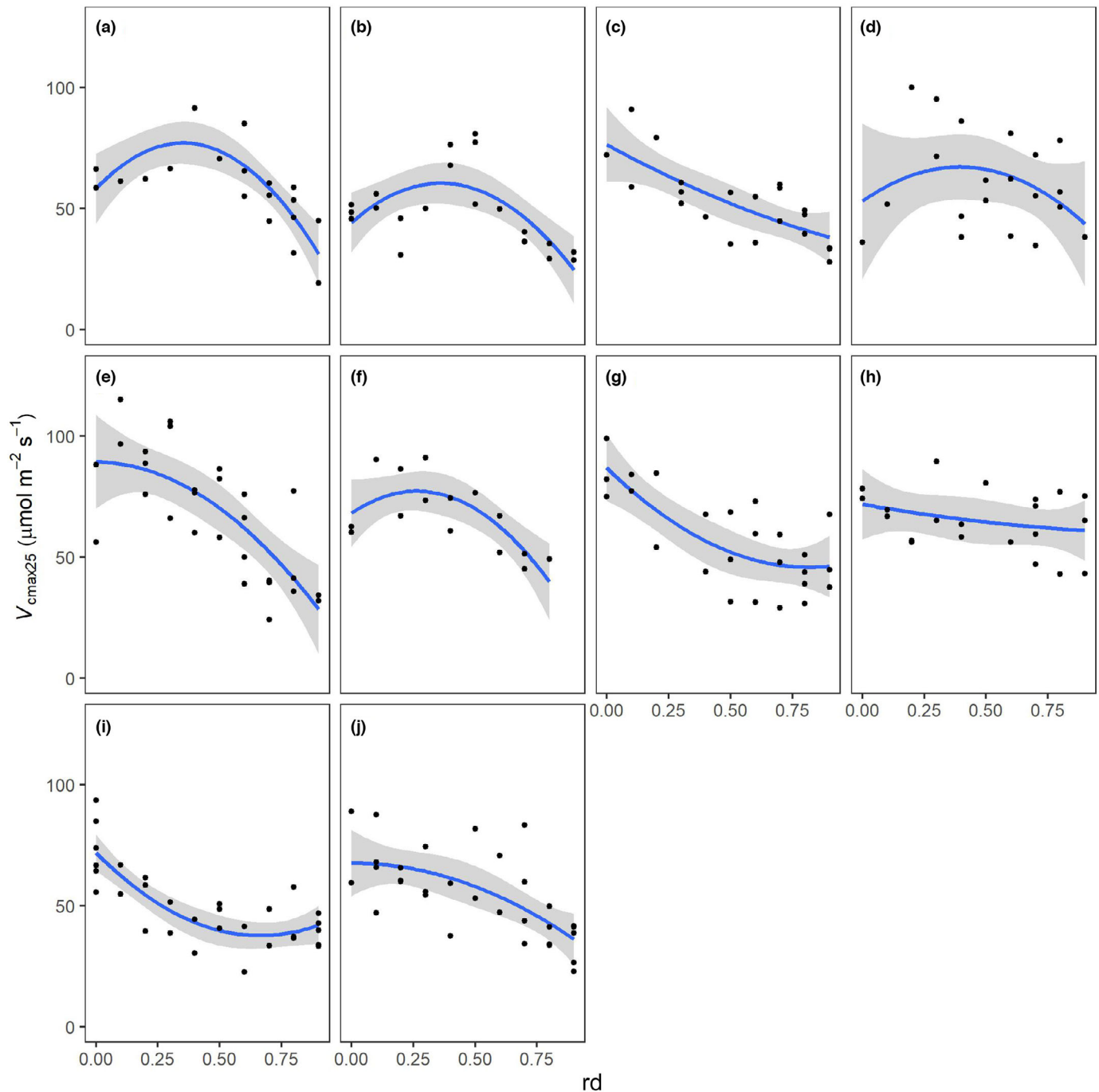


Fig. 7 Vertical gradients of the carboxylation capacity normalized to 25°C ($V_{\text{cmax}25}$) for each vertical profile a–j (corresponding to (a–j)), where the x-axis ordinates are the relative depth from the top of the canopy (rd). Each point represents an estimation of $V_{\text{cmax}25}$ by spectroscopy (Lamour *et al.*, 2021d). The blue line corresponds to the regression of a two-degree polynomial and the shaded interval represents the SE of the regression line.

Including a TPU limitation in the FvCB photosynthesis model did not change A and T (scenario 8 vs scenario 7), showing that TPU did not limit photosynthesis in our simulations.

Discussion

In this study, we measured vertical profiles of leaf physiological and chemical traits through the combined use of traditional measurements and leaf spectroscopy. This allowed us to estimate the

parameters at higher vertical resolution than previous studies that only used the slower traditional methods (Kitajima *et al.*, 1997; Carswell *et al.*, 2000; Domingues *et al.*, 2005, 2014; Kumagai *et al.*, 2006; Kosugi *et al.*, 2012). We tested some of the assumptions that are made within TBMs and evaluated their impact on simulated canopy scale A and T . We showed that the assumption of an exponential decrease in N_a and $V_{\text{cmax}25}$ with LAI did not adequately describe the observed gradients. Instead, we found a shallower decrease in trait values in the upper canopy than closer

Table 2 Vertical gradients of the ratio between the photosynthetic parameters and the maximum carboxylation capacity of rubisco normalized to 25°C ($V_{\text{cmax}25}$) or the nitrogen concentration per unit leaf area (N_a) obtained with Eqns 6 or 7 and rd as the vertical index.

P	Eqn	a	σ_α	b	σ_β	c	σ	AIC
$J_{\text{max}25} : V_{\text{cmax}25}$	6	1.96*** ± 0.02	0.10	0 ^{ns}	0.12	–	0.16	–164
$T_{\text{p}25} : V_{\text{cmax}25}$	7	0.115*** ± 0.01	0.027	–0.128*** ± 0.024	0.030	0.116*** ± 0.024	0.026	–997
$R_{\text{dark}25} : V_{\text{cmax}25}$	6	0.015*** ± 0.00	0.002	–0.008*** ± 0.001	0.002	–	0.004	–1822
$V_{\text{cmax}25} : N_a$	6	23.08*** ± 0.81	3.67	0 ^{ns}	4.78	–	6.20	1536
$J_{\text{max}25} : N_a$	6	44.44*** ± 1.30	7.56	0 ^{ns}	10.39	–	9.98	1761
$T_{\text{p}25} : N_a$	7	2.67*** ± 0.23	0.59	–2.93*** ± 0.69	0.69	2.53*** ± 0.69	0.75	556
$R_{\text{dark}25} : N_a$	6	0.36*** ± 0.02	0.06	–0.20*** ± 0.03	0.07	–	0.10	–347

a represents the intercept of the model, that is, the value of the ratio at the top of the canopy. σ_α is the SD associated with the random vertical profile effect (v) on a. b is the coefficient associated with rd and σ_β is the SD of the random effect of v on b. c represent the coefficient associated with rd² and σ is the SD of the residual. *, $P < 0.05$; **, $P < 0.01$; ***, $P < 0.001$; ns, not significant. The values after the sign ± represent the SE of the estimation. AIC, Akaike information criterion.

Table 3 Effect of the vertical indices z on the conductance parameters g_0 and g_1 of the USO conductance model (Eqn 9).

z	g_0	a	σ_α	g_1	b	σ_β	σ	AIC
–	0 ^{ns}	–	0.011	3.63*** ± 0.18	–	1.76	0.019	–495
rd	0 ^{ns}	0 ^{ns}	0.012	3.19*** ± 0.26	1.128* ± 0.513	1.73	0.019	–497
h	0 ^{ns}	0 ^{ns}	0.011	4.45*** ± 0.34	–0.052* ± 0.019	1.68	0.019	–500

a and b represent the fixed effect of z on g_0 and g_1 , respectively. σ_α and σ_β are the SD associated with the sample random effect on g_0 and g_1 , respectively, and σ is the SD of the residuals. The models including a vertical effect (z), either the relative depth from the top-of-canopy (rd), or the height (h) of the measurement improved the prediction ($P < 0.03$) compared with the simpler model without z (row with ‘–’ for z). The values after the sign ± represent the SE of the estimation. *, $P < 0.05$; **, $P < 0.01$; ***, $P < 0.001$; AIC, Akaike information criterion; ns, not significant.

to the ground. Contrary to assumptions, the ratio $R_{\text{dark}25} : V_{\text{cmax}25}$ at the ground was approximatively half that at the top-of-canopy. However, we confirmed that $V_{\text{cmax}25}$ closely followed the vertical gradients of N_a and that the ratio between $J_{\text{max}25}$ and $V_{\text{cmax}25}$ was constant within the canopy, consistent with model assumptions. We also found that g_1 showed a strong vertical variation, with much lower values near the top-of-canopy than near the ground. Terrestrial biosphere models currently assume there is no vertical gradient in stomatal parameters. Finally, we showed that simplifications made to represent the gradients of photosynthetic and conductance parameters result in underestimation of both A and T in this forest (Table 4).

Challenging the common assumption of an exponential decrease in N_a and the photosynthetic parameters with LAI

The exponential decrease in the photosynthetic parameters with LAI (Eqn 8) was obtained theoretically using an optimality approach where the photosynthetic capacity is optimized to the light conditions within-individual plant canopy (Field, 1983; Hirose & Werger, 1987; Chen *et al.*, 1993; Meir *et al.*, 2002; Lloyd *et al.*, 2010). However, this approach does not consider a possible limitation on leaf-scale photosynthesis by warmer and drier conditions typically found at vegetation top-of-canopy (Fetcher *et al.*, 1985; Miller *et al.*, 2021), as well as the water potential gradient from the soil to canopy top (Thomas & Bazaz, 1999; Buckley, 2021). The combination of saturating irradiance that maximizes A in the upper canopy layers is countered by greater stomatal limitation of A resulting from a higher VPD and

a potentially supra-optimal leaf temperature that in combination could explain the trend that we obtained in this study, that is, a moderate decrease at the top-of-canopy and a steeper one near the ground. In addition, most optimization approaches do not consider the impact of leaf age dynamics on these vertical gradients. Previous work has shown that in the tropics, leaf longevity varies substantially between shade and sunlit leaves, which also then impacts leaf physiology (Kitajima *et al.*, 1997; Reich *et al.*, 2004; Xu *et al.*, 2017; Wu *et al.*, 2019) and can also impact the theoretical shape of photosynthetic gradients (Kitajima *et al.*, 1997; Niinemets, 2007; Niinemets *et al.*, 2015).

In this study, we showed that rd better explained the vertical patterns than LAI for most of the traits (Tables S3, S4). Within an individual tree canopy, light availability is thought to be the main driver of leaf trait variation (Niinemets, 2010; Coble *et al.*, 2017) and LAI is used as a proxy for the light availability. Other studies have also shown that the height itself could explain the variability of leaf traits as it creates hydraulic constraints that lower the leaf turgor, reduce the cell expansion, and modulate the leaf morphology and physiology (Koch *et al.*, 2004; Cavaleri *et al.*, 2010; Zhang *et al.*, 2012). This would explain, in part, the lower LWC at the top-of-canopy. Furthermore, Thomas & Bazaz (1999) noted that the asymptotic height of species was a strong driver of variability in photosynthetic parameters. In addition, understory species are known to have low growth rates and low plasticity to changes in environmental conditions (Kitajima *et al.*, 1997; Valladares *et al.*, 1997). These effects could explain why understory species had a low $V_{\text{cmax}25}$, that was independent from the LAI, and this could explain the better description of the

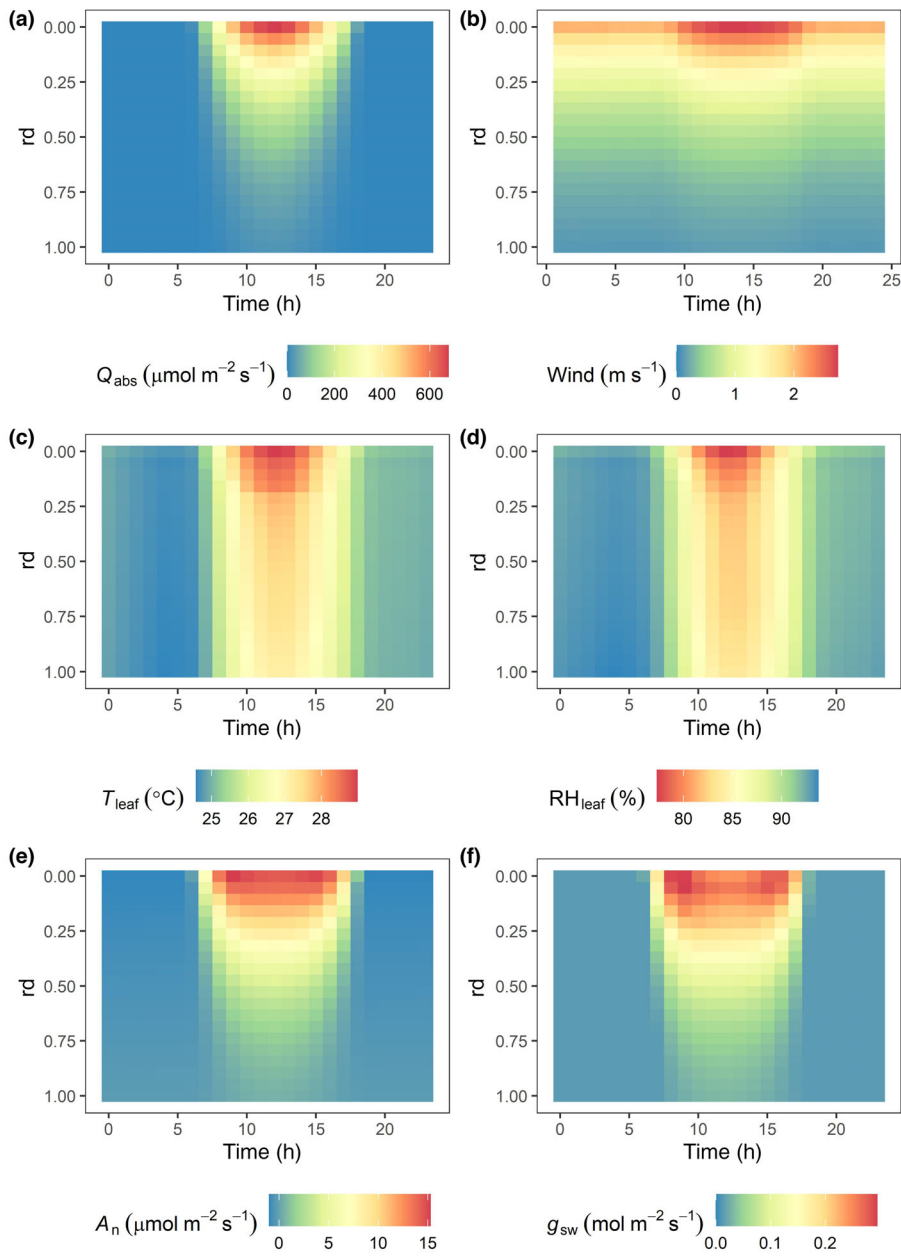


Fig. 8 Simulation of leaf gas exchange inside the canopy over the course of a day, where the y-axis ordinates are the relative depth from the top of the canopy (rd). For the simulations, the weather conditions at the top of the canopy were set to the average hourly values measured during the dry season (Fig. 1b). The leaf area index (LAI) on the ground was set to the average LAI measured in the forest (LAI = 6.2). The gradients of photosynthetic and conductance parameters followed the one measured during the measurement campaign (Scenario 7; Table 4). (a) Absorbed irradiance for an average leaf (Q_{abs}). (b) Wind speed inside the canopy. This variable was modeled using an exponential decrease from the top of the canopy (Buckley *et al.*, 2014). These data are important for the calculation of the boundary layer and the leaf energy balance. (c) Calculated leaf temperature (T_{leaf}). (d) Calculated leaf surface humidity (RH_{leaf}). (e) Net CO_2 assimilation rate (A) for an average leaf. Negative values correspond to cases in which the respiration rate was higher than the photosynthesis rate. (f) Leaf water conductance (g_{sw}) for an average leaf.

gradients using rd than LAI. Some TBMs include a minimum limit in V_{cmax25} and N_a values for the understory strata of dense canopy (Krinner *et al.*, 2005; Koven *et al.*, 2020). This approach seems reasonable considering our observations and is also supported by other work that showed a lower limit for N_a , and photosynthetic capacity that any species can attain (Meir *et al.*, 2002; Lloyd *et al.*, 2010).

Assumption of a constant ratio of J_{max25} , R_{dark25} , and T_{p25} with V_{cmax25} within the canopy

We showed that $J_{max25} : V_{cmax25}$ was constant within the canopy. This is in agreement with previous global studies which showed that the relationship between these two photosynthetic variables holds in multiple environmental conditions (Walker

et al., 2014). However, we also showed that $R_{dark25} : V_{cmax25}$ was dependent on vertical position and that leaves in the understory lose less CO_2 through respiration than expected compared with upper canopy leaves. Studies on the vertical variation of R_{dark25} are scarce in the tropics (Niinemets, 2014), which limits our ability to compare our results with other studies. However, our observations are consistent with the observations from Weerasinghe *et al.* (2014) in an Australian tropical forest that compared the respiration rate of top-of-canopy leaves with their counterpart near the ground on the same trees and other understory plants. They showed that the ratio of R_{dark25} to photosynthesis at saturation irradiance (A_{sat}) was 1.8 times higher at the top-of-canopy. Our canopy gradient measurements extend their finding through the canopy, with the same order of magnitude as what they measured. Our measurement of V_{cmax25} in place of A_{sat} should

Table 4 Effect of the vertical parametrization of the photosynthetic and conductance gradients on canopy-scale CO₂ assimilated (*A*, g CO₂ m⁻² yr⁻¹) and transpiration (*T*, l H₂O m⁻² yr⁻¹).

Scenario	Photosynthetic parameters	Conductance parameters	<i>A</i>	<i>T</i>
1. Original FATES parametrization	$V_{cmax25}(z) = 50e^{-0.142LAI(z)}$ $J_{max25}(z) = 1.67V_{cmax25}(z)$ $R_{dark25}(z) = 0.0142V_{cmax25}(z)$	$g_0(z) = 0.01$ $g_1(z) = 4.1$ $g_{sw,dark} = 0.01$	10 890 (–)	1045 (–)
2. Adapted top-of-canopy values and estimation of <i>k_n</i> based on Eqn 10	$V_{cmax25}(z) = 70.9e^{-0.174LAI(z)}$ $J_{max25}(z) = 133e^{-0.174LAI(z)}$ $R_{dark25}(z) = 1.04e^{-0.174LAI(z)}$	$g_0(z) = 0.01$ $g_1(z) = 4.1$ $g_{sw,dark} = 0.01$	12 776 (+17%)	1219 (+17%)
3. Adapted top-of-canopy values and estimation of <i>k_n</i> based on <i>V_{cmax25}</i> fitting ¹	$V_{cmax25}(z) = 70.9e^{-0.46rd(z)}$ $J_{max25}(z) = 133e^{-0.46rd(z)}$ $R_{dark25}(z) = 1.04e^{-0.46rd(z)}$	$g_0(z) = 0.01$ $g_1(z) = 4.1$ $g_{sw,dark} = 0.01$	12 358 (–3%)	1267 (+4%)
4. Adapted <i>k_n</i> for <i>R_{dark25}</i> ¹	$V_{cmax25}(z) = 70.9e^{-0.46rd(z)}$ $J_{max25}(z) = 133e^{-0.46rd(z)}$ $R_{dark25}(z) = 1.04e^{-1.04rd(z)}$	$g_0(z) = 0.01$ $g_1(z) = 4.1$ $g_{sw,dark} = 0.01$	13 968 (+13%)	1301 (+3%)
5. Measured gradients for <i>V_{cmax25}</i> , <i>J_{max25}</i> and <i>R_{dark25}</i>	$V_{cmax25}(z) = 70.9 - 6.7rd(z) - 30.3rd(z)^2$ $J_{max25}(z) = (133.0/70.9)V_{cmax25}(z)$ $R_{dark25}(z) = 1.04 - 0.78rd(z)$	$g_0(z) = 0.01$ $g_1(z) = 4.1$ $g_{sw,dark} = 0.01$	14 313 (+2%)	1324 (+2%)
6. Adapted top-of-canopy conductance parameters	$V_{cmax25}(z) = 70.9 - 6.7rd(z) - 30.3rd(z)^2$ $J_{max25}(z) = (133.0/70.9)V_{cmax25}(z)$ $R_{dark25}(z) = 1.04 - 0.78rd(z)$	$g_0(z) = 0.0$ $g_1(z) = 3.19$ $g_{sw,dark} = 0.013$	13 408 (–6%)	1038 (–22%)
7. Adapted conductance gradients	$V_{cmax25}(z) = 70.9 - 6.7rd(z) - 30.3rd(z)^2$ $J_{max25}(z) = (133.0/70.9)V_{cmax25}(z)$ $R_{dark25}(z) = 1.04 - 0.78rd(z)$	$g_0(z) = 0.0$ $g_1(z) = 3.19 + 1.13rd(z)$ $g_{sw,dark} = 0.013$	13 965 (+4%)	1257 (+21%)
8. Added triose phosphate utilization limitation	$V_{cmax25}(z) = 70.9 - 6.7rd(z) - 30.3rd(z)^2$ $J_{max25}(z) = (133.0/70.9)V_{cmax25}(z)$ $R_{dark25}(z) = 1.04 - 0.78rd(z)$ $T_{p25}(z) = 7.72 - 7.76(z) + 3.60rd(z)^2$	$g_0(z) = 0.0$ $g_1(z) = 3.19 + 1.13rd(z)$ $g_{sw,dark} = 0.013$	13 965 (0%)	1257 (0%)

An illustration of the data used to calculate *A* and *T* is given in Fig. 8 for scenario 7. The percentage given in the *A* and *T* columns corresponds to the changes in *A* and *T* between scenario *n* and scenario *n* – 1. *g_{sw,dark}* is the minimum conductance value used in the simulations.

¹The measured top-of-canopy values for *V_{cmax25}*, *J_{max25}*, and *R_{dark25}* corresponded to the values estimated by the best models in Table 1. Note that *k_n* for *V_{cmax25}*, *J_{max25}*, and *R_{dark25}* in scenarios 3 and 4 slightly differ from *b* estimated with the exponential model (Eqn 8) in Table 1. For example, *k_n* equals to 0.54 in Table 1 for *V_{cmax25}* while we use 0.46 in this table. This is because in Table 1, *a* and *b* were estimated simultaneously. In this table, we only fitted *k_n* (i.e. *b* in Table 1) and considered that *a* was fixed to the top-of-canopy value used in scenario 2, for consistency.

facilitate the implementation of such gradients in TBMs. One potential physiological explanation for higher *R_{dark25}*: *V_{cmax25}* in the upper canopy is the higher probability for photoprotection and photodamage at the top-of-canopy. This would result in higher respiratory costs, most notably for the recovery from photodamage through energetically expensive repair cycles (Aro *et al.*, 1993; Murata & Nishiyama, 2018). Interestingly, in an early version of FATES model, the understory vegetation was often predicted to die, in contradiction with empirical observations of slow growth rate and long lifetime (Koven *et al.*, 2020). FATES was therefore modified to allow plants to reduce their maintenance respiration when they reduce their carbon storage due to carbon starvation. Here, we showed an alternate explanation of the unexpected death of understory species in FATES, namely an overestimation of *R_{dark25}* in the lower canopy.

Assumption of constant *g₁* conductance parameter

Stomatal conductance increases with *A* (Eqn 2), and a high *g_{sw}* at the top-of-canopy is consistent with a greater investment in photosynthetic capacity at the top-of-canopy as observed previously (Fig. 6; Wong *et al.*, 1979; Roberts *et al.*, 1990; Rijkers *et al.*, 2000; Kosugi *et al.*, 2012). However, this does not reflect

the vertical variation of *g₁*, which is a key driver of uncertainty in TBMs (Ricciuto *et al.*, 2018).

Here, we showed that *g₁* decreased with increasing height. In terms of water-use efficiency, this means that leaves at the top-of-canopy are more water-use efficient and transpire less water to assimilate a given amount of carbon dioxide (Cowan & Farquhar, 1977; Medlyn *et al.*, 2011). It is usually assumed that *g₁* is constant in the canopy but recently, Buckley (2021) showed that optimality models that consider hydraulic and nitrogen limitations in addition to optimal water-use-efficiency, simulate higher *g₁* for shaded leaves compared with sunlit leaves – consistent with our observations. This is also consistent with observations of an increase in water-use efficiency with tree height commonly found using carbon isotope discrimination measurements (McDowell *et al.*, 2011; Brien *et al.*, 2017).

Domingues *et al.* (2014) studied vertical variation in the *g₁* parameter in an Amazonian forest. They found that *g₁* was vertically structured, with higher *g₁* in overstory trees than in mid-canopy or understory trees, the opposite relationship to the one we report here. They observed a low sensitivity of *g_{sw}* to changes in VPD_{leaf}, particularly for understory species, and, as a result, they suggested that Eqn 2 may not be suitable to model the stomatal behavior of these species. However, it is unclear whether

this effect impacted the estimation of g_1 or whether environmental and species differences explain the opposite relationship we found.

Our estimations of g_1 were made using steady-state measurements of leaf gas exchange on excised branches. Several studies have shown that excision can bias stomata measurement (Santiago & Mulkey, 2003; Missik *et al.*, 2021), yet other studies did not show an excision effect when sufficient time is given for stomata to fully stabilize and when the risk of embolism is reduced (Leakey *et al.*, 2006; Wolz *et al.*, 2017; Verryckt *et al.*, 2020; Davidson *et al.*, 2022). In this study, we took precautions to avoid xylem embolism by cutting the branches predawn, when the leaf water potential was typically > -0.8 mPa (Davidson *et al.*, 2023), and made measurements within the time period where we were confident that excision would not affect measured values of g_0 and g_1 (see Davidson *et al.*, 2023). Therefore, we believe it is unlikely that the gradients in g_1 we report here are due to excision, given that they are consistent with both theory and the isotopic measurements detailed above (McDowell *et al.*, 2011; Brien *et al.*, 2017; Buckley, 2021). One of the values of our work is that we provide measurements of g_1 variation with height, which describes a new axis of variation in g_1 that could be used to further parameterize stomatal models. This is in contrast to carbon discrimination techniques, which do not quantitatively estimate g_1 and cannot be directly used for model parametrization (Medlyn *et al.*, 2017). Further conductance measurements made at various heights in tropical forests, ideally on intact branches to avoid a possible excision effect, and in steady-state conditions, would help assess the generality of our findings.

Effect of these assumptions on canopy-scale fluxes of carbon and water

As highlighted by previous work (Zaehle *et al.*, 2005; Bonan *et al.*, 2011; Walker *et al.*, 2014), we found that accurate estimation of the photosynthetic parameters at the top-of-canopy is critical for model representation of A and T and that 15% of the total vegetation in the upper canopy accounted for nearly 50% of canopy scale A . However, once top-of-canopy parameterization is constrained, we showed that updating the k_n coefficient resulted in a marked modification of A and T . This was due to a decoupling between k_n for $V_{\text{cmax}25}$ and $R_{\text{dark}25}$. The $V_{\text{cmax}25} : R_{\text{dark}25}$ ratio was consistent with model assumptions at the top-of-canopy but almost half of model assumptions at the bottom of the canopy. Better representation of $R_{\text{dark}25}$ in TBMs is needed, not only to better account for vertical variation (this study and Weerasinghe *et al.*, 2014) but also to better account for nocturnal variation (Bruhn *et al.*, 2022). We also showed that the gradients for $V_{\text{cmax}25}$ and $R_{\text{dark}25}$ were not exponential, but also that changing the shape of the gradients only had a marginal effect on A and T (+2%). Further studies will be needed to validate whether this shape is observed in other sites, but it seems that even if the functional shape is not precisely represented, this has a low impact on the prediction of A and T . Finally, as with other leaf traits, we showed that it was key to correctly estimate g_1 at the top-of-canopy as well as its gradient.

Our study highlights some sources of uncertainty in models at the canopy scale and identifies key gradients that could be better represented in TBMs. The challenge for TBMs is to know whether the trends we observed are representative of other tropical sites, and indeed other biomes. There are high expectations from optimality models that prediction of photosynthetic parameters is possible from environmental variables (Ali *et al.*, 2016; Smith *et al.*, 2019; Franklin *et al.*, 2020). Such approaches were mainly used to predict photosynthetic parameters in different growth environments, but they could be expanded to include consideration of leaf longevity and hydraulic constraints to inform prognostic trait gradients within canopy. Other approaches could also make it possible to estimate g_1 gradients within canopies (Buckley, 2021). Currently, TBMs used in earth system models to predict future climate mainly consider geographically separated PFTs with usually low or no overlap within the same site (Fisher *et al.*, 2015, 2018). Recent dynamic vegetation models such as FATES have the ability to simulate different cohorts of plants with different parametrization that can cohabit and compete within the same site and that can occupy different strata in the canopy. In this condition, and even if each cohort is parametrized with Lloyd *et al.* (2010) model, the overall canopy-scale gradients could be different from an exponential decrease due to the mixing of the different cohorts vertically. To our knowledge, gradients predicted by such cohort models were not compared with experimental measurements. We welcome the use of our publicly available data by the community (Lamour *et al.*, 2021a,b,c) to compare gradients with predictions by optimal or cohort models.

Acknowledgements

We are grateful to the staff of the STRI for assistance with field logistics. We would also like to thank Edwin Andrades for his precise crane operating and trust and the forest guards Ernesto Camarena, Alberto Gonzales, and Anel Santamaria for their daily support at the forest site. This work was supported by the Next-Generation Ecosystem Experiments – Tropics project that is supported by the Office of Biological and Environmental Research in the Department of Energy, Office of Science, and through the United States Department of Energy contract no. DE-SC0012704 to Brookhaven National Laboratory. This manuscript has been co-authored by UT-Battelle, LLC under contract no. DE-AC05-00OR22725 with the US Department of Energy. The United States Government retains, and the publisher, by accepting the article for publication, acknowledges that the United States Government retains a nonexclusive, paid-up, irrevocable, world-wide license to publish or reproduce the published form of this manuscript, or allow others to do so, for United States Government purposes. The Department of Energy will provide public access to these results of federally sponsored research in accordance with the DOE Public Access Plan (<http://energy.gov/downloads/doe-public-access-plan>).












Competing interests

None declared.

Author contributions

JL, KJD, SPS and AR planned and designed the research. JL, KJD, KSE, JAA, OC, SPS and AR collected the data. JL and GLM analyzed the data. JL wrote the manuscript with contributions from KJD, KSE, GLM, QL, CDK, SJW, APW, SPS and AR.

ORCID

Jeremiah A. Anderson  <https://orcid.org/0000-0001-8925-5226>
 Kenneth J. Davidson  <https://orcid.org/0000-0001-5745-9689>
 Kim S. Ely  <https://orcid.org/0000-0002-3915-001X>
 Charles D. Koven  <https://orcid.org/0000-0002-3367-0065>
 Julien Lamour  <https://orcid.org/0000-0002-4410-507X>
 Gilles Le Moguédec  <https://orcid.org/0000-0002-7292-9121>
 Qianyu Li  <https://orcid.org/0000-0002-0627-039X>
 Alistair Rogers  <https://orcid.org/0000-0001-9262-7430>
 Shawn P. Serbin  <https://orcid.org/0000-0003-4136-8971>
 Anthony P. Walker  <https://orcid.org/0000-0003-0557-5594>
 S. Joseph Wright  <https://orcid.org/0000-0003-4260-5676>

Data availability

The data that support the findings of this study are provided in [Supporting Information](#) or publicly available in Lamour *et al.* (2021a,b,c).

References

- Akaike H. 1974. A new look at the statistical model identification. *IEEE Transactions on Automatic Control* 19: 716–723.
- Ali AA, Xu C, Rogers A, Fisher RA, Wullschleger SD, Massoud EC, Vrugt JA, Muss JD, McDowell NG, Fisher JB *et al.* 2016. A global scale mechanistic model of photosynthetic capacity (LUNA v.1.0). *Geoscientific Model Development* 9: 587–606.
- Aro E-M, Virgin I, Andersson B. 1993. Photoinhibition of photosystem II. Inactivation, protein damage and turnover. *Biochimica et Biophysica Acta (BBA) – Bioenergetics* 1143: 113–134.
- Ball JT, Woodrow IE, Berry JA. 1987. A model predicting stomatal conductance and its contribution to the control of photosynthesis under different environmental conditions. In: J Biggens, ed. *Progress in photosynthesis research*. Leiden, the Netherlands: Martinus Nijhoff, 221–224.
- Basset Y. 2003. *Studying forest canopies from above: the International Canopy Crane Network*. Balboa, Panama: Smithsonian Tropical Research Institute and UNEP. [WWW document] URL https://www.researchgate.net/publication/319506516_Studying_Forest_Canopies_from_Above_The_International_Canopy_Crane_Network [accessed September 2022].
- Bernacchi CJ, Pimentel C, Long SP. 2003. *In vivo* temperature response functions of parameters required to model RuBP-limited photosynthesis. *Plant, Cell & Environment* 26: 1419–1430.
- Bonan G, ed. 2019. Radiative transfer. In: *Climate change and terrestrial ecosystem modeling*. Cambridge, UK: Cambridge University Press, 228–259.
- Bonan GB, Lawrence PJ, Oleson KW, Levis S, Jung M, Reichstein M, Lawrence DM, Swenson SC. 2011. Improving canopy processes in the Community Land Model version 4 (CLM4) using global flux fields empirically inferred from FLUXNET data. *Journal of Geophysical Research* 116: G02014.
- Brienen RJW, Gloor E, Clerici S, Newton R, Arppe L, Boom A, Bottrell S, Callaghan M, Heaton T, Helama S *et al.* 2017. Tree height strongly affects estimates of water-use efficiency responses to climate and CO₂ using isotopes. *Nature Communications* 8: 288.
- Bruhn D, Newman F, Hancock M, Povlsen P, Slot M, Sitch S, Drake J, Weedon GP, Clark DB, Pagter M *et al.* 2022. Nocturnal plant respiration is under strong non-temperature control. *Nature Communications* 13: 5650.
- Buckley TN. 2021. Optimal carbon partitioning helps reconcile the apparent divergence between optimal and observed canopy profiles of photosynthetic capacity. *New Phytologist* 230: 2246–2260.
- Buckley TN, Martorell S, Diaz-Espejo A, Tomàs M, Medrano H. 2014. Is stomatal conductance optimized over both time and space in plant crowns? A field test in grapevine (*Vitis vinifera*). *Plant, Cell & Environment* 37: 2707–2721.
- Burnett AC, Anderson J, Davidson KJ, Ely KS, Lamour J, Li Q, Morrison BD, Yang D, Rogers A, Serbin SP. 2021. A best-practice guide to predicting plant traits from leaf-level hyperspectral data using partial least squares regression. *Journal of Experimental Botany* 72: 6175–6189.
- Carswell FE, Meir P, Wandelli EV, Bonates LCM, Kruijt B, Barbosa EM, Nobre AD, Grace J, Jarvis PG. 2000. Photosynthetic capacity in a central Amazonian rain forest. *Tree Physiology* 20: 179–186.
- Cavaleri MA, Oberbauer SF, Clark DB, Clark DA, Ryan MG. 2010. Height is more important than light in determining leaf morphology in a tropical forest. *Ecology* 91: 1730–1739.
- Chen J-L, Reynolds JF, Harley PC, Tenhunen JD. 1993. Coordination theory of leaf nitrogen distribution in a canopy. *Oecologia* 93: 63–69.
- Clark DB, Mercado LM, Sitch S, Jones CD, Gedney N, Best MJ, Pryor M, Rooney GG, Essery RLH, Blyth E *et al.* 2011. The Joint UK Land Environment Simulator (JULES), model description – Part 2: Carbon fluxes and vegetation dynamics. *Geoscientific Model Development* 4: 701–722.
- Coble AP, Fogel ML, Parker GG. 2017. Canopy gradients in leaf functional traits for species that differ in growth strategies and shade tolerance. *Tree Physiology* 37: 1415–1425.
- Cowan I, Farquhar G. 1977. Stomatal function in relation to leaf metabolism and environment. *Symposia of the Society for Experimental Biology* 31: 471–505.
- Davidson KJ, Lamour J, Rogers A, Ely KS, Li Q, McDowell NG, Pivovarov AL, Wolfe BT, Wright SJ, Zambrano A *et al.* 2023. Short-term variation in leaf-level water use efficiency in a tropical forest. *New Phytologist* 237: 2069–2087.
- Davidson KJ, Lamour J, Rogers A, Serbin SP. 2022. Late day measurement of excised branches results in uncertainty in the estimation of two stomatal parameters derived from response curves in *Populus deltoides* Bartr. × *Populus nigra* L. *Tree Physiology* 42: 1377–1395.
- De Pury DGG, Farquhar GD. 1997. Simple scaling of photosynthesis from leaves to canopies without the errors of big-leaf models. *Plant, Cell & Environment* 20: 537–557.
- Domingues TF, Berry JA, Martinelli LA, Ometto JP, Ehleringer JR. 2005. Parameterization of canopy structure and leaf-level gas exchange for an eastern Amazonian tropical rain forest (Tapajos National Forest, Para, Brazil). *Earth Interactions* 9: 1–23.
- Domingues TF, Martinelli LA, Ehleringer JR. 2014. Seasonal patterns of leaf-level photosynthetic gas exchange in an eastern Amazonian rain forest. *Plant Ecology & Diversity* 7: 189–203.
- Farquhar GD, von Caemmerer S, Berry JA. 1980. A biochemical model of photosynthetic CO₂ assimilation in leaves of C₃ species. *Planta* 149: 78–90.
- Fetcher N, Oberbauer SF, Strain BR. 1985. Vegetation effects on microclimate in lowland tropical forest in Costa Rica. *International Journal of Biometeorology* 29: 145–155.
- Field C. 1983. Allocating leaf nitrogen for the maximization of carbon gain: leaf age as a control on the allocation program. *Oecologia* 56: 341–347.
- Fisher RA, Koven CD, Anderegg WRL, Christoffersen BO, Dietze MC, Farrior CE, Holm JA, Hurtt GC, Knox RG, Lawrence PJ *et al.* 2018. Vegetation demographics in Earth System Models: a review of progress and priorities. *Global Change Biology* 24: 35–54.
- Fisher RA, Muszala S, Versteinstein M, Lawrence P, Xu C, McDowell NG, Knox RG, Koven C, Holm J, Rogers BM *et al.* 2015. Taking off the training wheels: the properties of a dynamic vegetation model without climate envelopes, CLM4.5(ED). *Geoscientific Model Development* 8: 3593–3619.

- Franklin O, Harrison SP, Dewar R, Farrior CE, Brännström Å, Dieckmann U, Pietsch S, Falster D, Cramer W, Loreau M *et al.* 2020. Organizing principles for vegetation dynamics. *Nature Plants* 6: 444–453.
- Franks PJ, Berry JA, Lombardozi DL, Bonan GB. 2017. Stomatal function across temporal and spatial scales: deep-time trends, land–atmosphere coupling and global models. *Plant Physiology* 174: 583–602.
- Franks PJ, Bonan GB, Berry JA, Lombardozi DL, Holbrook NM, Herold N, Oleson KW. 2018. Comparing optimal and empirical stomatal conductance models for application in Earth system models. *Global Change Biology* 24: 5708–5723.
- Gatti LV, Basso LS, Miller JB, Gloor M, Gatti Domingues L, Cassol HLG, Tejada G, Aragão LEOC, Nobre C, Peters W *et al.* 2021. Amazonia as a carbon source linked to deforestation and climate change. *Nature* 595: 388–393.
- Gregory LM, McClain AM, Kramer DM, Pardo JD, Smith KE, Tessmer OL, Walker BJ, Ziccardi LG, Sharkey TD. 2021. The triose phosphate utilization limitation of photosynthetic rate: out of global models but important for leaf models. *Plant, Cell & Environment* 44: 3223–3226.
- Hérault A, Lin Y-S, Bourne A, Medlyn BE, Ellsworth DS. 2013. Optimal stomatal conductance in relation to photosynthesis in climatically contrasting *Eucalyptus* species under drought. *Plant, Cell & Environment* 36: 262–274.
- Hetherington AM, Woodward FI. 2003. The role of stomata in sensing and driving environmental change. *Nature* 424: 901–908.
- Hikosaka K. 2016. Optimality of nitrogen distribution among leaves in plant canopies. *Journal of Plant Research* 129: 299–311.
- Hirose T, Werger MJA. 1987. Maximizing daily canopy photosynthesis with respect to the leaf nitrogen allocation pattern in the canopy. *Oecologia* 72: 520–526.
- Kitajima K, Mulkey SS, Wright SJ. 1997. Seasonal leaf phenotypes in the canopy of a tropical dry forest: photosynthetic characteristics and associated traits. *Oecologia* 109: 490–498.
- Koch GW, Sillett SC, Jennings GM, Davis SD. 2004. The limits to tree height. *Nature* 428: 851–854.
- Kosugi Y, Takanashi S, Yokoyama N, Philip E, Kamakura M. 2012. Vertical variation in leaf gas exchange parameters for a Southeast Asian tropical rainforest in Peninsular Malaysia. *Journal of Plant Research* 125: 735–748.
- Koven CD, Knox RG, Fisher RA, Chambers JQ, Christoffersen BO, Davies SJ, Detto M, Dietze MC, Faybishenko B, Holm J *et al.* 2020. Benchmarking and parameter sensitivity of physiological and vegetation dynamics using the Functionally Assembled Terrestrial Ecosystem Simulator (FATES) at Barro Colorado Island, Panama. *Biogeosciences* 17: 3017–3044.
- Krinner G, Viovy N, de Noblet-Ducoudré N, Ogée J, Polcher J, Friedlingstein P, Ciais P, Sitch S, Prentice IC. 2005. A dynamic global vegetation model for studies of the coupled atmosphere–biosphere system. *Global Biogeochemical Cycles* 19: GB1015.
- Kull O, Kruijt B. 1999. Acclimation of photosynthesis to light: a mechanistic approach. *Functional Ecology* 13: 24–36.
- Kumagai T, Ichie T, Yoshimura M, Yamashita M, Kenzo T, Saitoh TM, Ohashi M, Suzuki M, Koike T, Komatsu H. 2006. Modeling CO₂ exchange over a Bornean tropical rain forest using measured vertical and horizontal variations in leaf-level physiological parameters and leaf area densities. *Journal of Geophysical Research: Atmospheres* 111: D10107.
- Lamour J, Davidson KJ, Ely KS, Anderson J, Rogers A, Serbin SP. 2021a. Leaf spectral reflectance and transmittance, San Lorenzo, Panama, 2020 (v.1.0). *NGEE Tropics Data Collection*. doi: [10.15486/ngt/1781003](https://doi.org/10.15486/ngt/1781003).
- Lamour J, Davidson KJ, Ely KS, Anderson J, Rogers A, Serbin SP. 2021b. Leaf structural and chemical traits, and BNL field campaign sample details, San Lorenzo, Panama, 2020 (v.1.0). *NGEE Tropics Data Collection*. doi: [10.15486/ngt/1783737](https://doi.org/10.15486/ngt/1783737).
- Lamour J, Davidson KJ, Ely KS, Anderson J, Serbin SP, Rogers A. 2021c. Leaf gas exchange and fitted parameters, San Lorenzo, Panama, 2020 (v.1.0). *NGEE Tropics Data Collection*. doi: [10.15486/ngt/1781004](https://doi.org/10.15486/ngt/1781004).
- Lamour J, Davidson KJ, Ely KS, Anderson JA, Rogers A, Wu J, Serbin SP. 2021d. Rapid estimation of photosynthetic leaf traits of tropical plants in diverse environmental conditions using reflectance spectroscopy. *PLoS ONE* 16: e0258791.
- Lamour J, Davidson KJ, Ely KS, Le Moguédec G, Leakey ADB, Li Q, Serbin SP, Rogers A. 2022. An improved representation of the relationship between photosynthesis and stomatal conductance leads to more stable estimation of conductance parameters and improves the goodness-of-fit across diverse data sets. *Global Change Biology* 28: 3537–3556.
- Lamour J, Serbin SP. 2021. LEAFGASEXCHANGE: an R package for fitting and simulating leaf level gas exchange. *Zenodo*. doi: [10.5281/zenodo.4545818](https://doi.org/10.5281/zenodo.4545818).
- Leakey ADB, Bernacchi CJ, Ort DR, Long SP. 2006. Long-term growth of soybean at elevated [CO₂] does not cause acclimation of stomatal conductance under fully open-air conditions. *Plant, Cell & Environment* 29: 1794–1800.
- Leuning R. 1995. A critical appraisal of a combined stomatal–photosynthesis model for C₃ plants. *Plant, Cell & Environment* 18: 339–355.
- Leuning R. 2002. Temperature dependence of two parameters in a photosynthesis model. *Plant, Cell & Environment* 25: 1205–1210.
- Lin Y-S, Medlyn BE, Duursma RA, Prentice IC, Wang H, Baig S, Eamus D, de Dios VR, Mitchell P, Ellsworth DS *et al.* 2015. Optimal stomatal behaviour around the world. *Nature Climate Change* 5: 459–464.
- Lloyd J, Patiño S, Paiva RQ, Nardoto GB, Quesada CA, Santos AJB, Baker TR, Brand WA, Hilke I, Gielmann H *et al.* 2010. Optimisation of photosynthetic carbon gain and within-canopy gradients of associated foliar traits for Amazon forest trees. *Biogeosciences* 7: 1833–1859.
- Long SP, Bernacchi CJ. 2003. Gas exchange measurements, what can they tell us about the underlying limitations to photosynthesis? Procedures and sources of error. *Journal of Experimental Botany* 54: 2393–2401.
- McClain AM, Sharkey TD. 2019. Triose phosphate utilization and beyond: from photosynthesis to end product synthesis. *Journal of Experimental Botany* 70: 1755–1766.
- McDowell NG, Bond BJ, Dickman LT, Ryan MG, Whitehead D. 2011. Relationships between tree height and carbon isotope discrimination. In: Meinzer FC, Lachenbruch B, Dawson TE, eds. *Size- and age-related changes in tree structure and function*. Dordrecht, the Netherlands: Springer, 255–286.
- Medlyn BE, De Kauwe MG, Lin Y-S, Knauer J, Duursma RA, Williams CA, Arneeth A, Clement R, Isaac P, Limousin J-M *et al.* 2017. How do leaf and ecosystem measures of water-use efficiency compare? *New Phytologist* 216: 758–770.
- Medlyn BE, Duursma RA, Eamus D, Ellsworth DS, Prentice IC, Barton CVM, Crous KY, Angelis PD, Freeman M, Wingate L. 2011. Reconciling the optimal and empirical approaches to modelling stomatal conductance. *Global Change Biology* 17: 2134–2144.
- Meir P, Kruijt B, Broadmeadow M, Barbosa E, Kull O, Carswell F, Nobre A, Jarvis PG. 2002. Acclimation of photosynthetic capacity to irradiance in tree canopies in relation to leaf nitrogen concentration and leaf mass per unit area. *Plant, Cell & Environment* 25: 343–357.
- Migliavacca M, Musavi T, Mahecha MD, Nelson JA, Knauer J, Baldocchi DD, Perez-Priego O, Christiansen R, Peters J, Anderson K *et al.* 2021. The three major axes of terrestrial ecosystem function. *Nature* 598: 468–472.
- Miller BD, Carter KR, Reed SC, Wood TE, Cavaleri MA. 2021. Only sun-lit leaves of the uppermost canopy exceed both air temperature and photosynthetic thermal optima in a wet tropical forest. *Agricultural and Forest Meteorology* 301–302: 108347.
- Missik JEC, Oishi AC, Benson MC, Meretsky VJ, Phillips RP, Novick KA. 2021. Performing gas-exchange measurements on excised branches – evaluation and recommendations. *Photosynthetica* 59: 61–73.
- Mitchard ETA. 2018. The tropical forest carbon cycle and climate change. *Nature* 559: 527–534.
- Muir CD. 2019. TEALAVES: an R package for modelling leaf temperature using energy budgets. *AoB Plants* 11: plz054.
- Murata N, Nishiyama Y. 2018. ATP is a driving force in the repair of photosystem II during photoinhibition. *Plant, Cell & Environment* 41: 285–299.
- Niinemets Ü. 2007. Photosynthesis and resource distribution through plant canopies. *Plant, Cell & Environment* 30: 1052–1071.
- Niinemets Ü. 2010. A review of light interception in plant stands from leaf to canopy in different plant functional types and in species with varying shade tolerance. *Ecological Research* 25: 693–714.

- Niinemets Ü. 2014. Improving modeling of the 'dark part' of canopy carbon gain. *Tree Physiology* 34: 557–563.
- Niinemets Ü, Keenan TF, Hallik L. 2015. A worldwide analysis of within-canopy variations in leaf structural, chemical and physiological traits across plant functional types. *New Phytologist* 205: 973–993.
- Norman J. 1979. *Modelling the complete crop canopy*. St Joseph, MI, USA: American Society of Agricultural Engineers, 249–277.
- Oleson K, Lawrence D, Bonan G, Drewniak B, Huang M, Koven C, Levis S, Li F, Riley W, Subin Z *et al.* 2013. *Technical description of v.4.5 of the Community Land Model (CLM)*. Boulder, CO, USA: NCAR Technical Notes.
- Osnas JLD, Katabuchi M, Kitajima K, Wright SJ, Reich PB, Van Bael SA, Kraft NJB, Samaniego MJ, Pacala SW, Lichstein JW. 2018. Divergent drivers of leaf trait variation within species, among species, and among functional groups. *Proceedings of the National Academy of Sciences, USA* 115: 5480–5485.
- Parker GG. 2020. Tamm review: leaf area index (LAI) is both a determinant and a consequence of important processes in vegetation canopies. *Forest Ecology and Management* 477: 118496.
- Paton S. 2022. Monthly summary San Lorenzo crane. *Smithsonian.figshare* doi: 10.25573/data.10059518.v28.
- Pinheiro J, Bates D. 2000. *Mixed-effects models in S and S-PLUS*. New York, NY, USA: Springer Science & Business Media.
- R Core Team. 2020. *R: a language and environment for statistical computing*. Vienna, Austria: R Foundation for Statistical Computing.
- Reich PB, Ellsworth DS, Uhl C. 1995. Leaf carbon and nutrient assimilation and conservation in species of differing successional status in an oligotrophic Amazonian forest. *Functional Ecology* 9: 65–76.
- Reich PB, Uhl C, Walters MB, Prugh L, Ellsworth DS. 2004. Leaf demography and phenology in Amazonian rain forest: a census of 40 000 leaves of 23 tree species. *Ecological Monographs* 74: 3–23.
- Ricciuto D, Sargsyan K, Thornton P. 2018. The impact of parametric uncertainties on biogeochemistry in the E3SM land model. *Journal of Advances in Modeling Earth Systems* 10: 297–319.
- Rijkers T, Pons TL, Bongers F. 2000. The effect of tree height and light availability on photosynthetic leaf traits of four neotropical species differing in shade tolerance. *Functional Ecology* 14: 77–86.
- Roberts J, Cabral OM, De Aguiar LF. 1990. Stomatal and boundary-layer conductances in an Amazonian terra firme rain forest. *Journal of Applied Ecology* 27: 336–353.
- Rogers A, Kumarathunge DP, Lombardozzi DL, Medlyn BE, Serbin SP, Walker AP. 2021. Triose phosphate utilization limitation: an unnecessary complexity in terrestrial biosphere model representation of photosynthesis. *New Phytologist* 230: 17–22.
- Rogers A, Medlyn BE, Dukes JS, Bonan G, Von Caemmerer S, Dietze MC, Kattge J, Leakey AD, Mercado LM, Niinemets Ü. 2017a. A roadmap for improving the representation of photosynthesis in Earth system models. *New Phytologist* 213: 22–42.
- Rogers A, Serbin SP, Ely KS, Sloan VL, Wullschlegel SD. 2017b. Terrestrial biosphere models underestimate photosynthetic capacity and CO₂ assimilation in the Arctic. *New Phytologist* 216: 1090–1103.
- Santiago LS, Mulkey SS. 2003. A test of gas exchange measurements on excised canopy branches of ten tropical tree species. *Photosynthetica* 41: 343–347.
- Serbin SP, Gower ST, Ahl DE. 2009. Canopy dynamics and phenology of a boreal black spruce wildfire chronosequence. *Agricultural and Forest Meteorology* 149: 187–204.
- Serbin SP, Wu J, Ely KS, Kruger EL, Townsend PA, Meng R, Wolfe BT, Chlus A, Wang Z, Rogers A. 2019. From the Arctic to the tropics: multibiome prediction of leaf mass per area using leaf reflectance. *New Phytologist* 224: 1557–1568.
- Smith NG, Keenan TF, Colin Prentice I, Wang H, Wright IJ, Niinemets Ü, Crous KY, Domingues TF, Guerrieri R, Yoko Ishida F *et al.* 2019. Global photosynthetic capacity is optimized to the environment. *Ecology Letters* 22: 506–517.
- Sperry J. 2013. Cutting-edge research or cutting-edge artefact? An overdue control experiment complicates the xylem refilling story. *Plant, Cell & Environment* 36: 1916–1918.
- Sullivan MJP, Lewis SL, Affum-Baffoe K, Castilho C, Costa F, Sanchez AC, Ewango CEN, Hubau W, Marimon B, Monteagudo-Mendoza A *et al.* 2020. Long-term thermal sensitivity of Earth's tropical forests. *Science* 368: 869–874.
- Thomas SC, Bazzaz FA. 1999. Asymptotic height as a predictor of photosynthetic characteristics in Malaysian rain forest trees. *Ecology* 80: 1607–1622.
- Valladares F, Allen MT, Pearcy RW. 1997. Photosynthetic responses to dynamic light under field conditions in six tropical rainforest shrubs occurring along a light gradient. *Oecologia* 111: 505–514.
- Verryckt LT, Van Langenhove L, Ciais P, Courtois EA, Vicca S, Peñuelas J, Stahl C, Coste S, Ellsworth DS, Posada JM *et al.* 2020. Coping with branch excision when measuring leaf net photosynthetic rates in a lowland tropical forest. *Biotropica* 52: 608–615.
- Walker AP, Beckerman AP, Gu L, Kattge J, Cernusak LA, Domingues TF, Scales JC, Wohlfahrt G, Wullschlegel SD, Woodward FI. 2014. The relationship of leaf photosynthetic traits – V_{cmax} and J_{max} – to leaf nitrogen, leaf phosphorus, and specific leaf area: a meta-analysis and modeling study. *Ecology and Evolution* 4: 3218–3235.
- Weerasinghe LK, Creek D, Crous KY, Xiang S, Liddell MJ, Turnbull MH, Atkin OK. 2014. Canopy position affects the relationships between leaf respiration and associated traits in a tropical rainforest in Far North Queensland. *Tree Physiology* 34: 564–584.
- Wolz KJ, Wertin TM, Abordo M, Wang D, Leakey ADB. 2017. Diversity in stomatal function is integral to modelling plant carbon and water fluxes. *Nature Ecology & Evolution* 1: 1292–1298.
- Wong S, Cowan I, Farquhar G. 1979. Stomatal conductance correlates with photosynthetic capacity. *Nature* 282: 424–426.
- Wu J, Rogers A, Albert LP, Ely K, Prohaska N, Wolfe BT, Oliveira RC Jr, Saleska SR, Serbin SP. 2019. Leaf reflectance spectroscopy captures variation in carboxylation capacity across species, canopy environment and leaf age in lowland moist tropical forests. *New Phytologist* 224: 663–674.
- Wu J, Serbin SP, Ely KS, Wolfe BT, Dickman LT, Grossiord C, Michaletz ST, Collins AD, Detto M, McDowell NG *et al.* 2020. The response of stomatal conductance to seasonal drought in tropical forests. *Global Change Biology* 26: 823–839.
- Xu X, Medvigy D, Joseph Wright S, Kitajima K, Wu J, Albert LP, Martins GA, Saleska SR, Pacala SW. 2017. Variations of leaf longevity in tropical moist forests predicted by a trait-driven carbon optimality model. *Ecology Letters* 20: 1097–1106.
- Zaehle S, Sitch S, Smith B, Hatterman F. 2005. Effects of parameter uncertainties on the modeling of terrestrial biosphere dynamics. *Global Biogeochemical Cycles* 19: GB3020.
- Zhang Y, Zheng Q, Tyree MT. 2012. Factors controlling plasticity of leaf morphology in *Robinia pseudoacacia* L. I: height-associated variation in leaf structure. *Annals of Forest Science* 69: 29–37.

Supporting Information

Additional Supporting Information may be found online in the Supporting Information section at the end of the article.

Fig. S1 Vertical gradients of $J_{\text{max}25}$ by vertical profile.

Fig. S2 Vertical gradients of T_{p25} by vertical profile.

Fig. S3 Vertical gradients of $R_{\text{dark}25}$ by vertical profile.

Fig. S4 Vertical gradients of leaf mass per surface area by vertical profile.

Fig. S5 Vertical gradients of N_a by vertical profile.

Fig. S6 Vertical gradients of leaf water content by vertical profile.

Fig. S7 Vertical gradients of the ratio between the photosynthetic parameters $J_{\max 25}$, T_{p25} , $R_{\text{dark}25}$, and $V_{\text{cmax}25}$.

Fig. S8 Vertical gradients of the ratio between the photosynthetic parameters $V_{\text{cmax}25}$, $J_{\max 25}$, T_{p25} , $R_{\text{dark}25}$, and the leaf nitrogen concentration expressed on a leaf area basis.

Fig. S9 Effect of the relative depth from the top-of-canopy (rd) on the conductance parameter g_1 of the USO model.

Fig. S10 Scenarios of photosynthetic parameters used to parameterize the canopy-scale model.

Table S1 Species measured in the vertical profiles.

Table S2 List of datasets used to build the N_a and leaf water content reflectance models.

Table S3 Effect of the vertical index on the prediction of the leaf composition traits.

Table S4 Effect of the vertical index on the prediction of the leaf photosynthetic traits.

Please note: Wiley is not responsible for the content or functionality of any Supporting Information supplied by the authors. Any queries (other than missing material) should be directed to the *New Phytologist* Central Office.